JPL NO. 9950-332

DRL NO. 74/DRD NO. SE

DOE/JPL - 955089 - 80/76

LINE ITEM NO. 7

SILICON SOLAR CELL PROCESS DEVELOPMENT, FABRICATION AND ANALYSIS

FIFTH QUARTERLY REPORT

FOR PERIOD COVERING

1 OCTOBER 1979 TO 31 DECEMBER 1979

By

H.I. YOO, P.A. ILES AND F.F. HO

JPL CONTRACT NO. 955089

OPTICAL COATING LABORATORY, INC.
PHOTOELECTRONICS DIVISION
15251 EAST DON JULIAN ROAD
CITY OF INDUSTRY, CA 91746

"The JPL Low-Cost Silicon Solar Array Project is sponsored by the U.S. Department of Energy and forms part of the Solar Photovoltaic Conversion Program to initiate a major effect toward the development of low-cost solar arrays. This work was performed for the Jet Propulsion Laboratory, California Institute of Technology by agreement between NASA and DOE."

ABSTRACT

Evaluation was performed for three sheet silicon forms:

(a) EFG (RH) Multi-Ribbon (Mobil-Tyco)

(b) Dendritic Web (Westinghouse)

(c) Cast Silicon by HEM (Crystal Systems),

A number of solar cell fabrication processes were used and average AM0 efficiencies obtained were as follows:

(a)	*EFG Cells*	
	(i) BSF Process	*7.3%*
	*(ii) Grain Boundary Passivation**	*7.5%*
(b)	*Dendritic Web Cells*	
	(i) Shallow Junction Plus BSF	*11.1%*
	(ii) BSF Plus Back Surface Reflector (BSR)	*12.8%*
(c)	*HEM Cells*	
	(i) Standard Process	*9.5%*

The junction shunting problems caused by the BSF process were analyzed using ion microprobe/SIMS and an optical microscope, indicating aluminum contamination of the front junction area in the form of alloy pits.

**Refer to Section A, 1.0 for details.*

TABLE OF CONTENTS

LIST OF FIGURES

LIST OF TABLES

I. INTRODUCTION

This program investigates, develops and utilizes technologies appropriate and necessary for improving the efficiency of solar cells made from various unconventional silicon sheet materials. During this reporting period, work has progressed in fabrication and characterization of solar cells from EFG (RH) multi-ribbon, dendritic webs and cast silicon by HEM. Solar cells were fabricated using various process modifications, such as shallow junction formation, BSF, back surface reflector (BSR), suface etching and texturizing, gettering by mechanical damage and diffusion glass and grain boundary passivation.

The solar cell parameters measured included open circuit voltage, short circuit current, curve fill factor, and conversion efficiency (all taken under AM0 illumination). Additional measurements under AM1 conditions have been included, for direct evaluation and to collect information on the AM1/AM0 conversion factors for the various sheet materials. Also, measurement for typical cells included spectral response and minority carrier diffusion length. No data on dark I-V characteristics and photoresponse by fine light spot scanning was included since the results were similar to those reported in earlier technical reports. The obtained results were compared to the properties of cells made from conventional single crystalline Czochralski silicon with an emphasis on statistical evaluation. Increased emphasis was given toward modifying the process to yield increased performance.

The BSF process is a well-known and widely used technique to improve silicon solar cell performance by increasing V_{oc} *and* I_{sc}. *A common method to form a BSF is to screen print aluminum paste, followed by an alloy formation step at an elevated temperature. This process can provide advantages in solar cell performance, but in practice can also give possible yield problems, mainly due to junction shunting or leakage. Work has progressed to identify the problems using an ion microprobe/SIMS and an optical microscope.*

II. TECHNICAL DISCUSSION

A. EFG (RH) MULTI-RIBBON SOLAR CELL

1.0 SOLAR CELL FABRICATION

The EFG ribbons delivered were RH furnace grown with multiple dies. Measured resistivity was around 1 ohm-cm with p-type conductivity. The Fourth Quarterly Report (1) gave detailed information on the starting blanks and performance results of solar cells fabricated by the standard process and by the higher efficiency process. In this reporting period, efforts have continued in an attempt to improve cell efficiency by using various modified process steps. The ribbon blanks (2x2 cm) were sliced and divided into two groups; one for the modified process and the other for the unmodified process. In each case the CZ silicon blanks of about the same resistivity were added and processed in parallel with the EFG blanks. This provided a direct check of the effect of each additional processing step. Details of the process modification are described in the following section and performance results are given in Section 2.0.

Surface Etching Tests

In a previous report (1), it was reported that a short-time $POCl_3$ diffusion followed by a thin surface etch-off step, prior to cell junction formation, showed an increase in cell output. However, the result did not indicate whether the $POCl_3$ diffusion or the surface etching step was responsible for the enhanced output. As a consequence, a simple surface etching test was carried out; the EFG blanks were placed in plastic

carriers and dipped in a planar etch solution for 30 seconds. Standard solar cells were fabricated using the blanks.

Surface Texturizing

Surface texturizing processes using orientation-dependent etching techniques have been developed to reduce the reflection of incident light from the front surface, leading to an improvement in solar cell efficiency. Single crystal solar cells fabricated in this fashion have shown a significant increase in short-circuit current under illumination. An experiment was performed to assess the feasibility and the effect of surface texturizing process on the performance of solar cells made from the EFG ribbons.

The texture etching apparatus used in this experiment included a hot plate and a solution container. EFG ribbon blanks were placed vertically in a plastic carrier, and immersed for about 20 minutes in a texturizing solution (2% NaOH + 8% Isopropyl Alcohol in DI water) maintained at $80^{o}C$. A partially textured surface was observed, indicating a large variation in crystal orientation throughout the entire surface of the EFG ribbons.

Gettering by Diffusion Glass

The objective of this experiment was to determine whether a phospho-silicate glass gettering step could improve cell output by removing the undesired impurities, possibly introduced by the dies and the growth chamber. Thus, tests were carried out to grow a phospho-silicate glass layer on the wafer surface using a standard $POCl_3$ diffusion at $875^{o}C$. Deposition of the glass layer lasted for about forty (40) minutes and the glass layer and a thin surface layer (about 1-2 μm) of the EFG were removed before the

standard solar cell process. Note: No extra heat treatment was used after the deposition of the diffused layer.

Gettering by Mechanical Damage

It is well known that the mechanical damage on the silicon surface can getter bulk impurities and defects when proper process steps are used. EFG ribbons were sand blasted on the back side and then cleaned in Aqua Regia to remove possible contaminants from the sand blasting step. Solar cells were fabricated by forming junctions both front and back, etching-off the back damaged layer and evaporating contacts. A standard diffusion cycle, contact pattern and AR coating were used for this process.

Grain Boundary Passivation

Attempts were made to enhance carrier collection efficiency for the EFG ribbons by utilizing a preferential diffusion along grain boundary at low temperature. This scheme (so called grain boundary passivation) offers the possibility of an increase in conversion efficiency of the EFG cells. The test was carried out by deposition of a dopant source (20 minutes $POCl_3$ diffusion at 875^{o}C), followed by drive-in at low temperature (600^{o}C for 24 hours in N_2 atmosphere). Finally, the glass layer was removed and a standard process was used to complete the cells. Note: Efforts to passivate grain boundaries of Wacker "Silso" wafer were tried using a spin-on diffusion source. The results were reported in the First Quarterly Report of this contract.

Back Surface Field Process

Solar Cells were fabricated using the BSF process described in Appendix III of reference (2).

2.0 SOLAR CELL PERFORMANCE AND CHARACTERIZATION

Characteristics Under Illumination

Finished solar cells had evaporated SiO AR coatings and about 90% active area with Ti-Pd-Ag metallization. Solar cell parameters, such as Isc, Voc, CFF and η, were measured under an AM0 simulator at 25°C test block temperature. Descriptions of the simulator and the light intensity calibration methods used are discussed in Appendix IV of reference (2) for the AM0 conditions.

Solar cell parameters of individual EFG cells having undergone a surface treatment (two batches of plain surface etching and one batch of surface texturizing) are given in Appendix III and Table 1 summarizes the results. The table suggests that there is no significant change in performance between cells with the treatment and the cells without the treatment. An average AM0 eficiency of EFG control is around 6%.

Solar cell parameters from other process modifications, such as gettering diffusion glass, grain boundary passivation or the BSF process (see Section 1.0 for the details), are summarized in Table 2. Solar cells from the gettering test did not show any improvment in efficiency. However, solar cells from grain boundary passivation (GP) and the BSF process did show significant improvement in efficiency, indicating an average AM0 efficiency of 7.5% for the GP process cells and 7.3% for the BSF cells. A few

BSF cells still showed junction shunting problems (see Appendix III for individual cell data) and the statistics in the table did not include these shunted cells. Solar cells utilizing surface mechanical damage gettering gave poor performance, low Voc and CFF, mainly due to insufficient removal of the damaged layer. As a consequence, no electrical data are reported on these cells.

Spectral Response

Absolute spectral response (A/W) was made using a filter wheel set-up (see Appendix V of reference 2) for the details). Response versus wavelength of the EFG solar cells from the process modifications is given in Figure 1 for the surface etching, Figure 2 for the BSF, and Figure 3 for the GP. Overall response of the EFG cells from the surface etching was about the same as the respone of the standard EFG cells described in the previous report (1). However, response of the BSF and the GP process cells showed significant improvement in long wavelength response, especially the cell with the GP process. This suggests that there might be a possible impurity redistribution in the bulk, or curing of crystallographic defects from a relatively long period of heat treatment at low temperature (600°C for 24 hours).

TABLE 1

SUMMARY OF PARAMETERS OF SOLAR CELLS FABRICATED FROM EFG (RH) MULTI-RIBBONS AFTER SURFACE TREATMENTS

		SURFACE ETCHING		SURFACE TEXTURIZING	
		EFG	Control[2]	EFG	Control[2]
V_{oc} (mV)	Average	514	505	519	512
	Standard Deviation	12	12	---	---
	Range	502-538	495-511	516-524	506-517
J_{sc} (mA/cm^2)	Average	23.2	23.5	21.9	21.2
	Standard Deviation	2.4	1.6	---	---
	Range	19.8-26.3	22.7-25.1	21.4-22.6	20.7-21.9
CFF (%)	Average	66	69	70	69
	Standard Deviation	5	4	---	---
	Range	58-73	65-74	70-71	66-72
η (%)	Average	5.8	6.0	5.9	5.6
	Standard Deviation	0.5	0.6	---	---
	Range	5.2-6.5	5.8-7.0	5.7-6.2	5.1-5.8

NOTES:
1. Cells with standard process (2x2 cm, SiO AR coating) measured under AM0 conditions at 25°C test block temperature.
2. Control cells mean EFG cells fabricated without surface treatment.
3. Sample Size: Surface Etching - EFG: 11 cells
   EFG Control: 6 cells

TABLE 2

SUMMARY OF PARAMETERS OF SOLAR CELLS FABRICATED FROM EFG (RH) MULTI-RIBBONS USING PROCESS MODIFICATIONS

		GETTERING	G.P.*	BSF
V_{oc} (mV)	Average	503	537	532
	Standard Deviation	9	14	7
	Range	487-516	516-550	519-540
J_{sc} (mA/cm^2)	Average	22.4	25.9	26.2
	Standard Deviation	0.8	1.5	0.8
	Range	21-23.3	23.8-27.8	24.8-27.3
CFF (%)	Average	70	73	71
	Standard Deviation	5	3	4
	Range	59-74	68-75	61-74
η (%)	Average	5.8	7.5	7.3
	Standard Deviation	0.6	0.8	0.6
	Range	4.7-6.3	6.2-8.2	6.0-7.9

NOTES: 1. Cells (2x2 cm) with SiO AR coating measured under AM0 conditons at 25°C test block temperature.
2. Sample Size: Gettering - 6 cells
G.P.* - 6 cells
BSF - 10 cells

*Grain boundary passivation

FIGURE 1

SPECTRAL RESPONSE OF SOLAR CELLS FROM EFG (RH); SURFACE ETCHING PROCESS

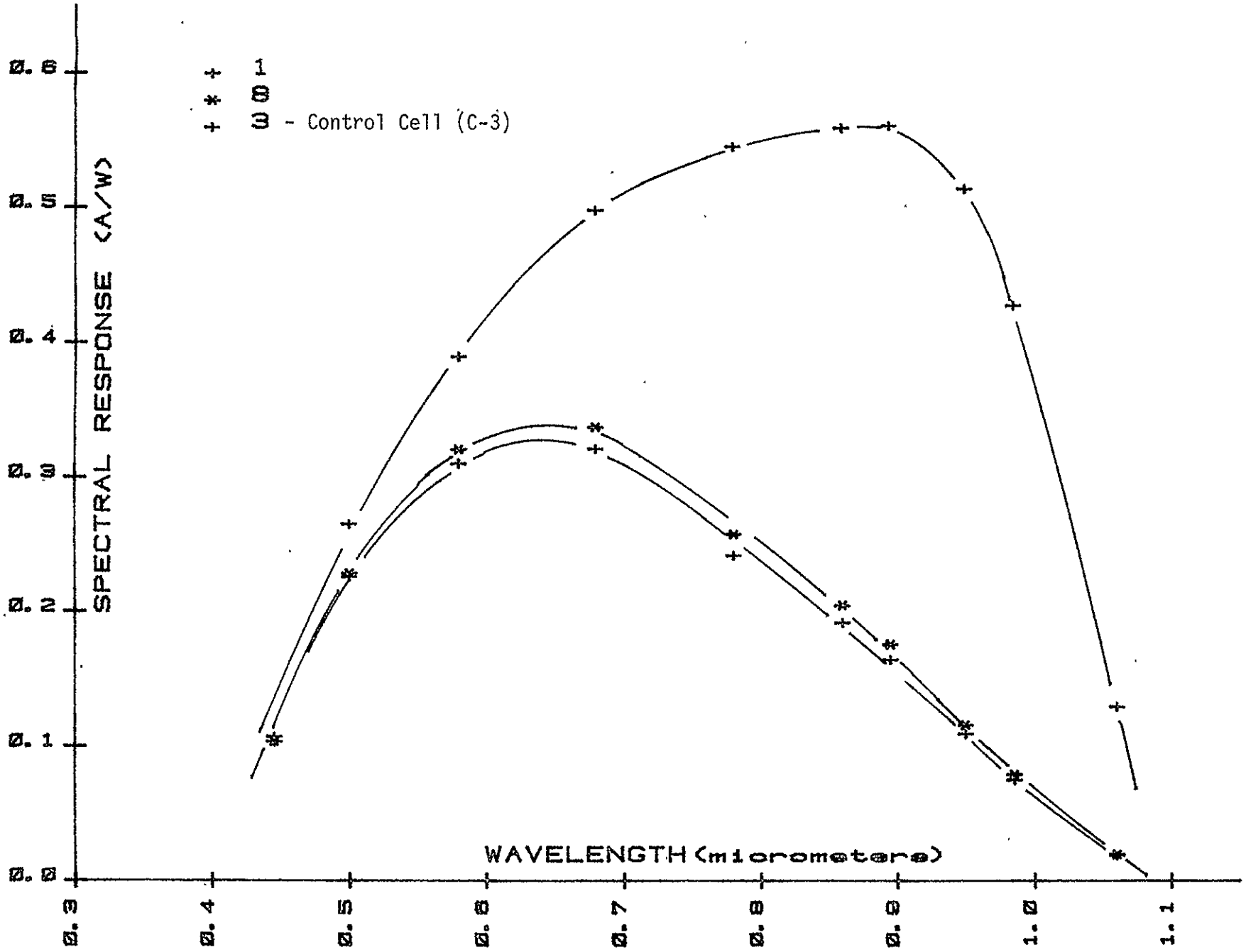

FIGURE 2

SPECTRAL RESPONSE OF SOLAR CELLS FROM EFG (RH) RIBBONS; BSF PROCESS

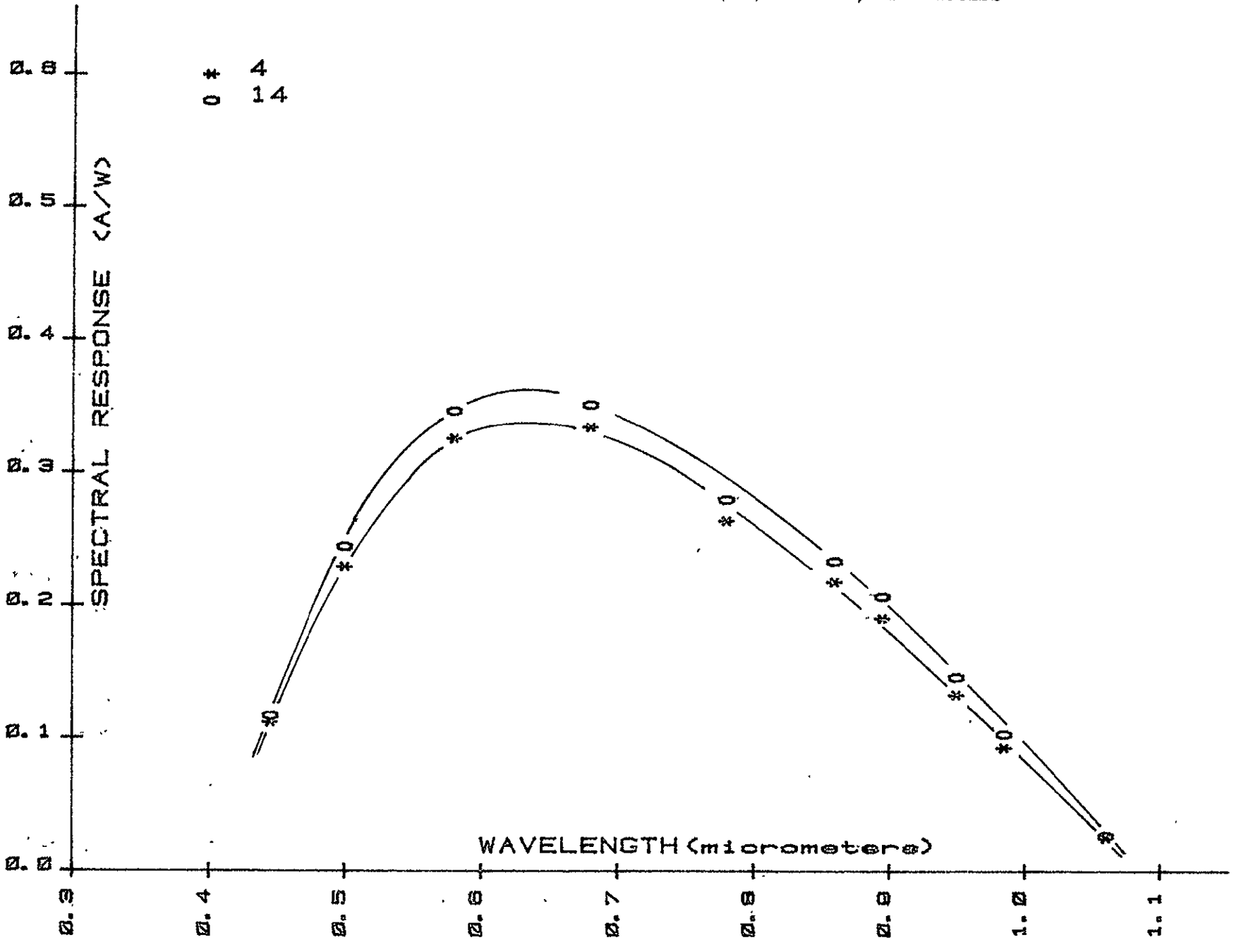

FIGURE 3

SPECTRAL RESPONSE OF SOLAR CELLS FROM EFG (RH) RIBBONS;
GRAIN BOUNDARY PASSIVATION PROCESS

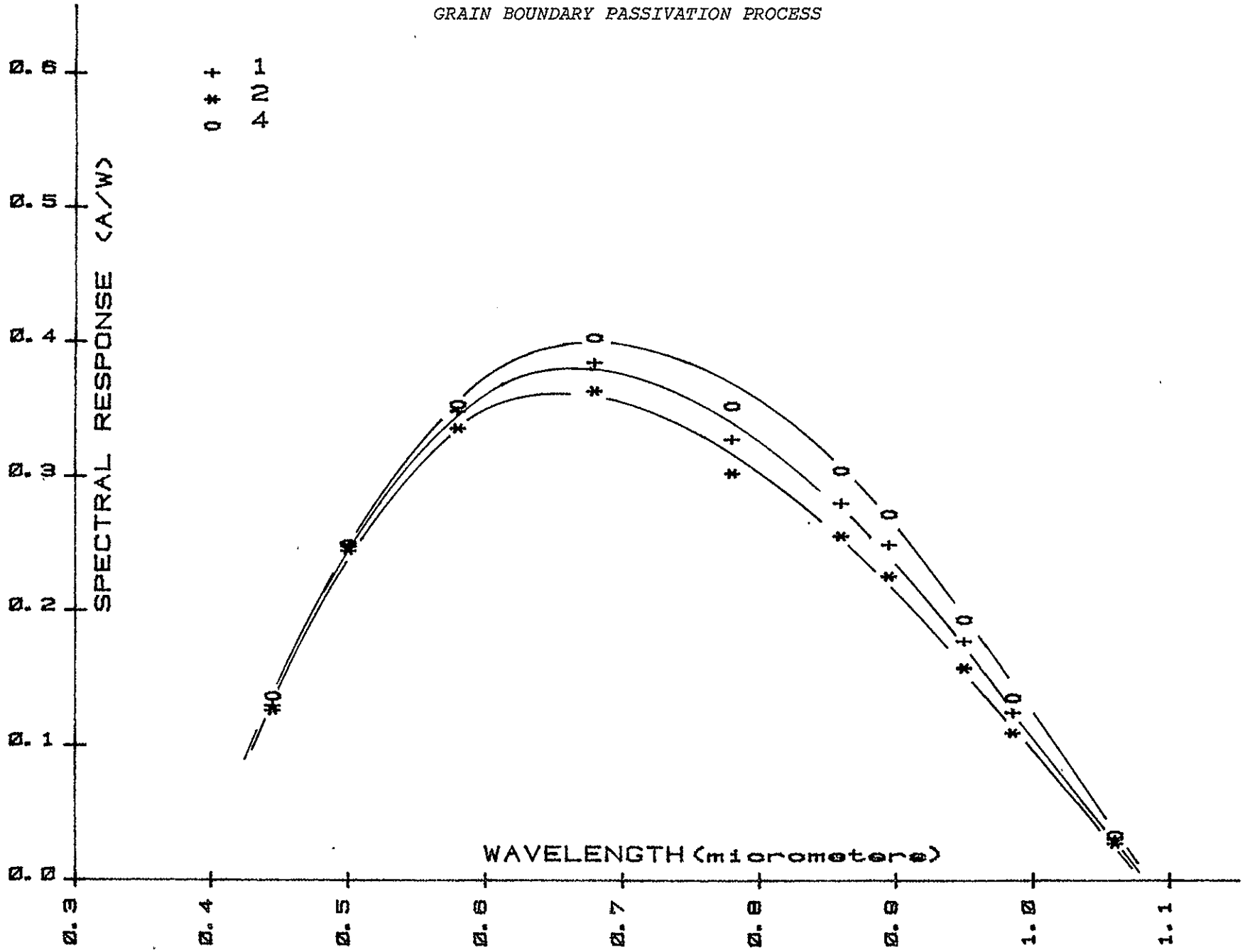

B. DENDRITIC WEB SOLAR CELLS

1.0 SOLAR CELL FABRICATION

Standard process solar cells were fabricated from dendritic webs and the performance results have been reported in reference (1). During this reporting period, work has progressed to fabricate solar cells utilizing shallow junction, fine grid line patterns, BSF and BSR processes.

Solar cells 1" x 1" were fabricated using the BSF process. A shallow junction was formed to improve blue response (a sheet resistance about 50 ohm/square) and the front grid lines were applied using fine photomask patterns, which gave about 92% active area. Finally, a multi-layer AR (MLAR) coating was evaporated the cells to minimize surface reflection.

Efforts were directed found making the best-state-of-the-art solar cells from dendritic webs on 2x2 cm blanks. The key process steps used were the same as above, with the addition of a back suface reflector (BSR).

2.0 SOLAR CELL PERFORMANCE AND CHARACTERIZATION

Characteristics Under Illumination

Solar cell parameters, such as Isc, Voc, CFF and η, were measured under AM0 and AM1 conditons at 25^{o}C test block temperature. Individual electrical data are given in Appendix IV. Descriptions of the simulators and light intensity calibration methods used are discussed in Appendix IV of reference (2) for the AM0 conditions and Appendix II of reference (1) for the AM1 conditions.

Table 3 summarizes the important parameters of high performance web cells; "A" for the 1" x 1" web cells with shallow junction, MLAR coating and BSF process and "B" for the best-state-of-the-art process cells (2x2 cm) with the addition of BSR process to "A". Dendritic web solar cells from both "A" and "B" showed significant improvement in efficiency over the standard web solar cells (see previous report (1)); an average AM0 efficiency of 10.1% for the standard cells versus 11.1% for the web "A" cells and 12.8% for the web "B" cells. A web cell from the "B" process showed an AM0 efficiency as high as 14.2%, which corresponds to measured AM1 efficiency of 15.5%.

Spectral Response

Absolute spectral response (A/W) was made using a filter wheel set-up (see Appendix V of reference (2) for the details). Response versus wavelength is given in Figure 4 for the 1" x 1" web cells and in Figure 5 for the 2x2 cm cells. Figure 4 indicates that significant improvement in blue response is noticed compared with the standard cells reported earlier. One web cell (#4 cell) shows lower overall response than the other (#1 cell), suggesting an inconsistency in silicon sheet quality. Czochralski control cells of about the same resistivity showed higher response in the long wavelength region. Figure 5 shows similar results from the best-state-of-the-art process (2x2 cm). The response at wavelength 0.45 μm indicates a quantum efficiency higher than 100%. This could either be due to a measurement error due to low light level at this wavelength along with a reduced response from the standard cell, or possibly to impact ionization.

TABLE 3

SUMMARY OF PARAMETERS OF SOLAR CELLS FABRICATED FROM DENDRITIC WEBS USING PROCESS MODIFICATIONS

		A		B
		WEB	CONTROL	WEB
V_{oc} (mV)	Average	564	584	585
	Standard Deviation	23	---	11
	Range	520-588	580-588	569-604
J_{sc} (mA/cm^2)	Average	36.2	37.6	39.4
	Standard Deviation	1.7	---	0.9
	Range	32.9-37.8	37.5-37.8	37.8-41.0
CFF (%)	Average	73	75	75
	Standard Deviaton	2	---	3
	Range	71-77	73-77	70-78
η (%)	Average	11.1	12.1	12.8
	Standard Deviation	1.1	---	0.7
	Range	9.4-12.6	11.9-12.6	11.6-14.2

NOTES:
1. A: 1" x 1" cells with shallow junction, MLAR coating and BSF process.
   B: 2 x 2 cm cells with shallow junction, MLAR, BSF and BSR process.
2. Cells measured under AM0 conditions at 25°C test block temperature.
3. Sample Size: A - Web: 7 cells
   Control: 3 cells
   B - Web: 10 cells
4. Control cells mean cells fabricated from CZ silicon of about the same resistivity.

FIGURE 4

SPECTRAL RESPONSE OF SOLAR CELLS FROM DENDRITIC WEB; 1"x1" CELLS WITH SHALLOW JUNCTION AND BSF PROCESS

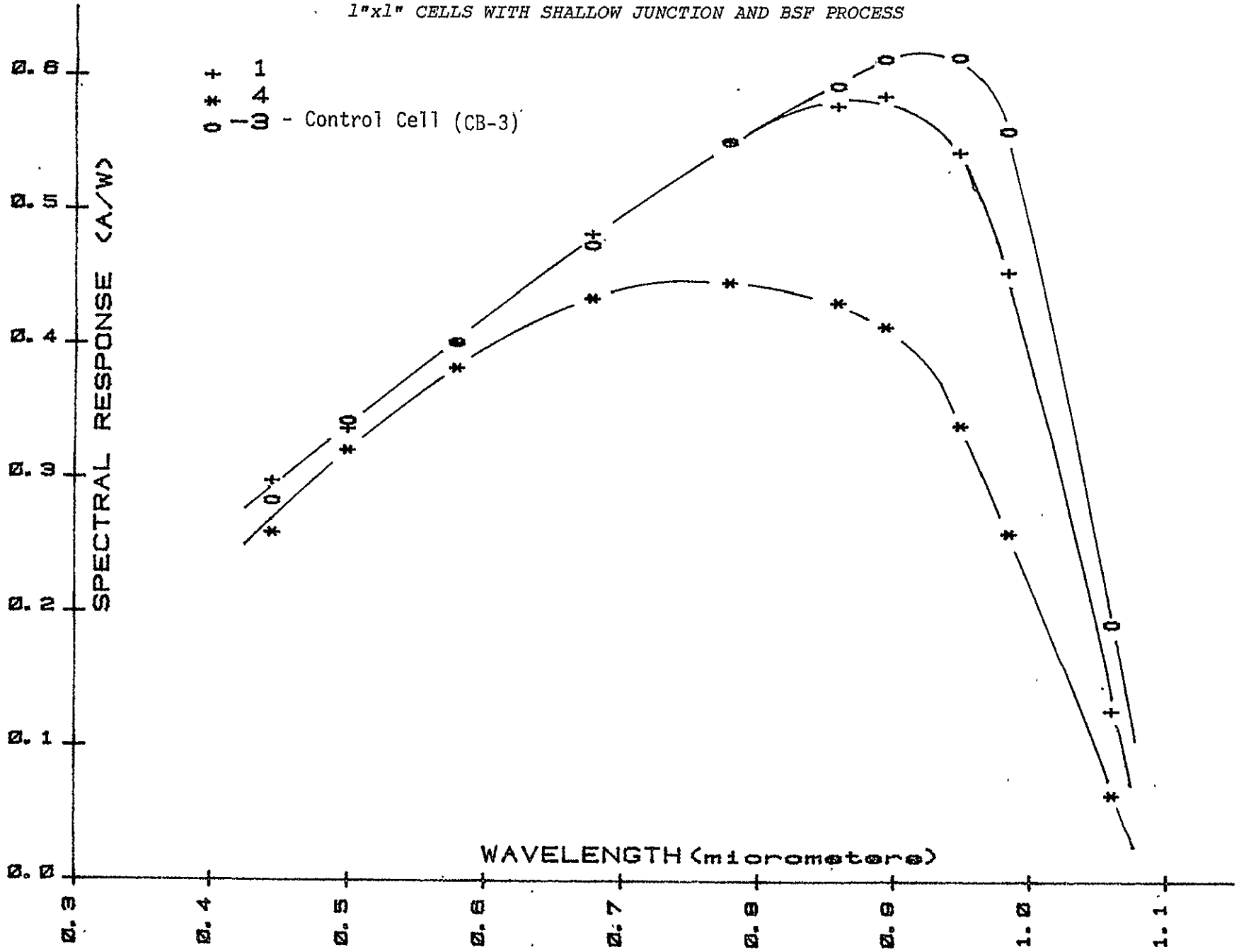

FIGURE 5

SPECTRAL RESPONSE OF SOLAR CELLS FROM DENDRITIC WEB;
2x2 CM CELLS WITH SHALLOW JUNCTION, BSF AND BSR PROCESS

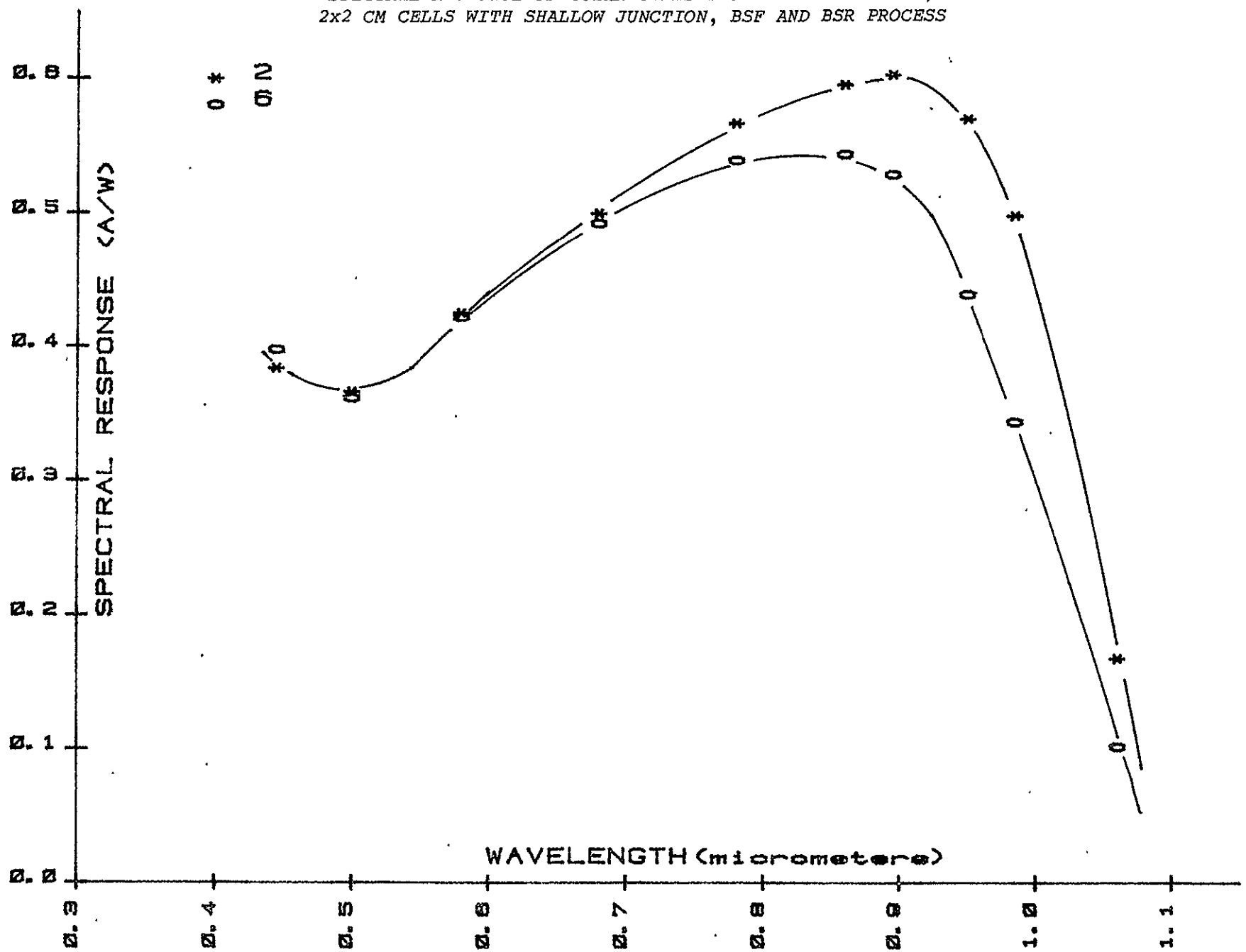

C. HEM SOLAR CELLS

1.0 SOLAR CELL FABRICATION

Blanks (2x2 cm) were prepared by slicing the cast silicon blocks using an ID saw. The silicon blocks were prepared from three casting experiments at Crystal Systems; run numbers 342C, 349C and 314C. Measured resistivity of the sliced blanks ranged between 0.5 ohm-cm and 1.5 ohm-cm with p-type conductivity. One cast ingot (Run #314C) showed resistivity variations between 0.8 and 1.5 ohm-cm from end-to-end of the 3" block. Approximately half of the blanks showed some degree of polycrystallinity while the other half was single crystal. Minority carrier diffusion lengths (SPV method) were in the range 30 to 80 μm.

The thickness of the starting blanks was 16 mils which were thinned down to about 13 mils using a planar etching solution. Two batches of solar cells were fabricated using the standard process (see Appendix III of reference (2) for the details of the process); one batch contained single crystalline HEM and the other batch was polycrystalline HEM.

2.0 SOLAR CELL PERFORMANCE AND CHARACTERIZATION

Characteristics Under Illumination

Solar cell parameters, such as Isc, Voc, CFF and η, were measured under AM0 and AM1 solar simulation at 25°C test block temperature. Electrical data sheets in Appendix V give detailed information on individual cells; single crystal HEM cells (1st batch) and polycrystalline HEM cells (2nd batch). Table 4 summarizes the cell parameters of the two batch processes

showing an average AM0 efficiency of 9.5% for the single crystalline HEM cells and 7.6% for the polycrystalline HEM cells. Significant difference in performance between the two batches was due to the difference in CFF; an average CFF of 73% for the single crystal HEM cells versus 63% for the poly HEM cells. Low CFF of the poly HEM was partly due to the inclusions observed in the bulk HEM material. Figure 6 shows microscopic photographs of the inclusions (or possibly precipitates); (a) for the precipitates at the grain boundary and (b) for the precipitates in the bulk. Note, the inclusions were observed on the poly section of ingot run number 314C, specifically at the position close to the last part of solification.

Selected solar cells were tested under AM1 conditions and Table 5 summarizes the results. Single crystalline HEM solar cells showed an average AM1 efficiency of 10.8%, while that of the control cells showed 12.5%. Table 6 gives AM0-AM1 conversion ratio of Jsc and η for both the HEM solar cells and the control cells. The table indicates that AM1 efficiency of the HEM and the control cell is approximately 13-14% higher than AM0 efficiency.

Spectral Response

Absolute spectral response (A/W) was measured using a filter wheel set-up (refer to Appendix V of reference (2) for the details). Responses are plotted in Figure 7 for the single crystalline HEM cells and in Figure 8 for the poly HEM cells. In both cases, a good cell and a bad cell were shown in the figures and significant difference in long wavelength

response is noticed: long wavelength response of the control cell is considerably lower than the previous control cells which this could possibly be due to measurement error.

TABLE 4

SUMMARY OF PARAMETERS OF SOLAR CELLS FABRICATED FROM HEM; STANDARD PROCESS

		HEM (Single)	HEM (Poly)	CZ Control
V_{oc} (mV)	Average	584	584	593
	Standard Deviation	8	8	1
	Range	574-598	570-599	592-595
J_{sc} (mA/cm^2)	Average	30.1	28.2	33.4
	Standard Deviation	1.4	2.0	0.4
	Range	28.3-32.5	24.3-31.3	32.8-33.8
CFF (%)	Average	73	63	76
	Standard Deviation	4	7	2
	Range	60-77	51-73	74-78
η (%)	Average	9.5	7.6	11.1
	Standard Deviation	0.8	0.9	0.3
	Range	7.6-10.6	6.7-9.4	10.8-11.6

NOTES: 1. Cells (2x2 cm) with SiO AR coating measured under AM0 conditions at 25°C test block temperature.
2. Sample size: HEM (single): 20 cells
HEM (poly): 14 cells
CZ Control: 5 cells

TABLE 5

COMPARISON OF HEM SOLAR CELL PARAMETERS UNDER AM0 AND AM1 ILLUMINATION CONDITIONS

		HEM		CONTROL	
		AM0	AM1	AM0	AM1
V_{oc} (mV)	Average	583	579	593	587
	Standard Deviation	7	8	---	---
	Range	578-598	571-591	592-594	586-588
J_{sc} (mA/cm^2)	Average	30.0	25.9	33.5	27.8
	Standard Deviation	5.6	1.2	---	---
	Range	28.5-31.8	24.5-27.3	33.3-33.8	27.5-28.0
CFF (%)	Average	74	72	75	77
	Standard Deviation	2	2	---	---
	Range	71-77	71-74	74-76	76-78
η(%)	Average	9.5	10.8	11.1	12.5
	Standad Deviation	0.6	0.7	---	---
	Range	9.0-10.2	10-11.8	10.8-11.3	12.2-12.8

NOTES:
1. Data based on selected sample measurement for AM1.
2. Solar cells with SiO AR coating measured at 25^{o}C test block temperature.
3. See Appendix IV of reference (2) for AM0 simulation conditions and Appendix V of reference (1) for AM1 simulation conditions.

TABLE 6

AN AM0-AM1 CONVERSION RATIO OF SHORT CIRCUIT CURRENT DENSITY (J_{sc}) AND EFFICIENCY (η) OF HEM SOLAR CELLS

	J_{sc}, AM0/AM1	n, AM1/AM0
HEM	1.16	1.14
CONTROL	1.21	1.13

NOTES:
1. Data based on selected sample measurement for AM1.
2. Solar cells with SiO AR coating measured at 25°C test block temperature.
3. See Appendix IV of Reference (2) for AM0 simulation conditions and Appendix II of reference (1) for AM1 simulation conditions.

(a)

(b)

FIGURE 6

MICROSCOPIC PHOTOGRAPHS OF INCLUSIONS (OR PRECIPITATES) FOUND IN HEM SILICON (CRYSTAL SYSTEMS RUN #314C); 200X

(a) Precipitates at the grain boundary
(b) Precipitates in the bulk

FIGURE 7

SPECTRAL RESPONSE OF SOLAR CELLS FABRICATED FROM SINGLE CRYSTALLINE HEM; STANDARD PROCESS

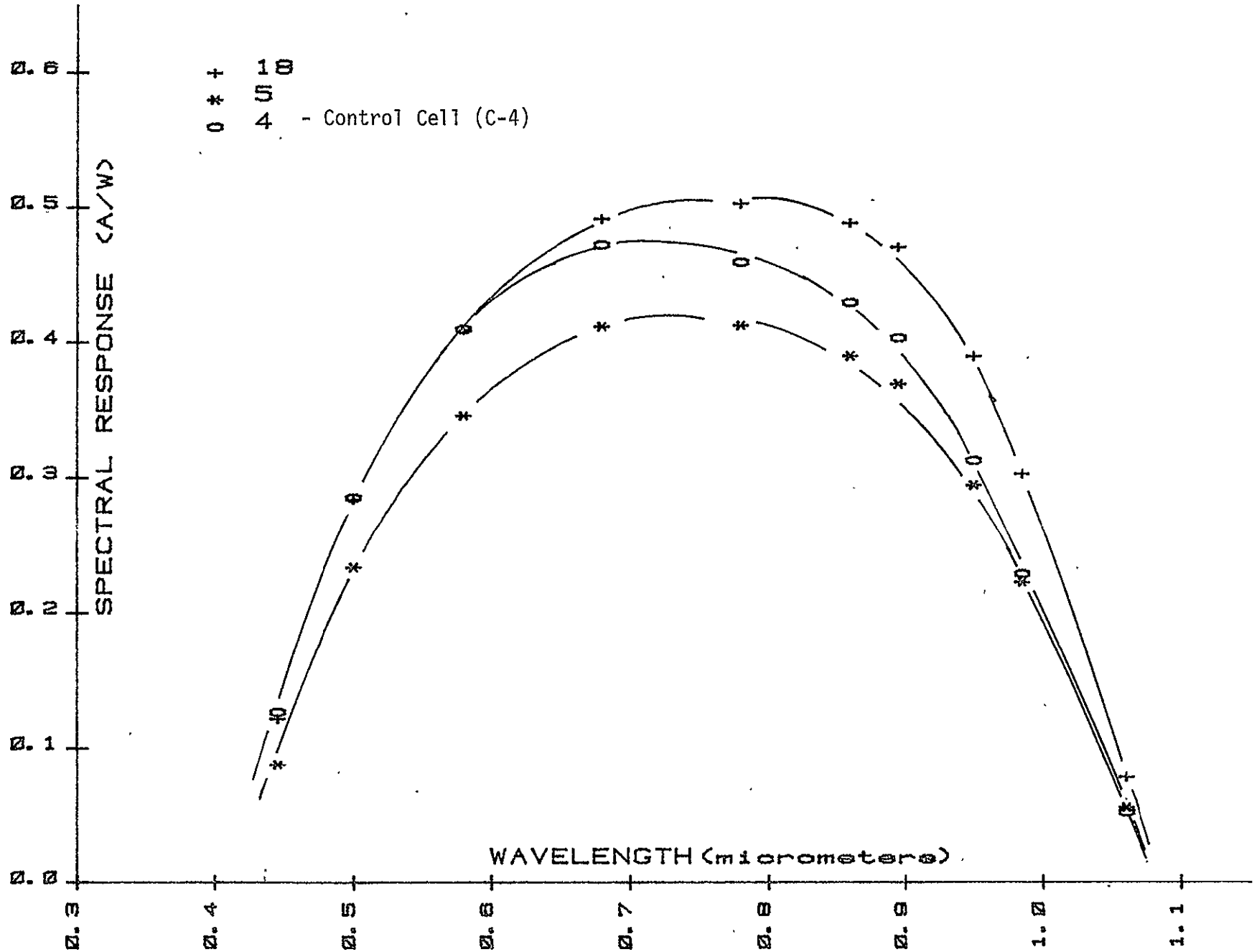

FIGURE 8

SPECTRAL RESPONSE OF SOLAR CELLS FABRICATED FROM POLYCRYSTALLINE HEM; STANDARD PROCESS

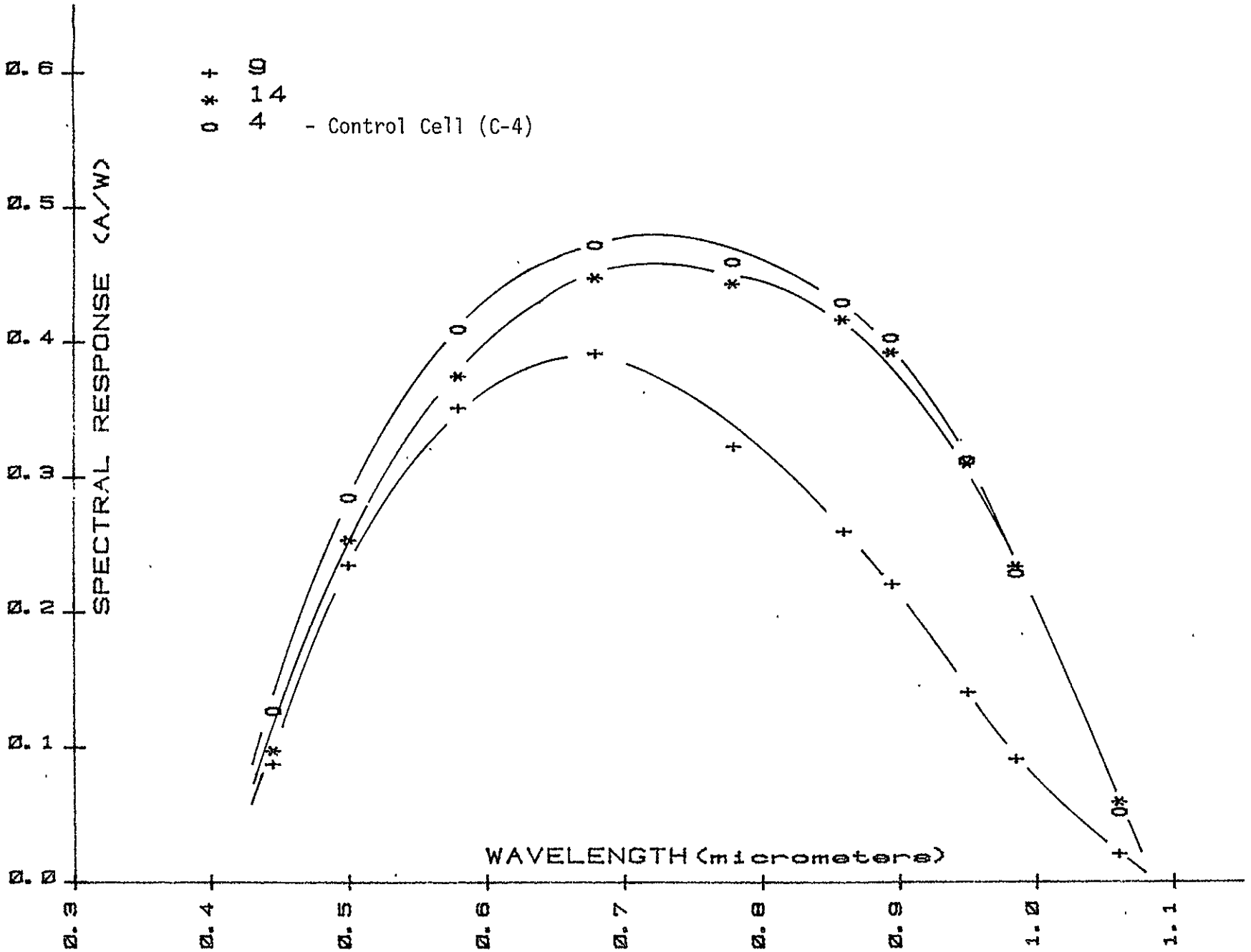

D. BSF PROCESS DEVELOPMENT

The BSF process is a well-known and widely used technique to improve silicon solar cell performance by increasing open circuit voltage and short circuit current. A common method to form a BSF is to screen print aluminum paste, followed by an alloy formation step at an elevated temperature, typically around 800°C, for a short period. This process can provide advantages in solar cell performance, but in practice can also give possible yield problems, mainly due to junction shunting or leakage. Typical illumination characteristics of solar cells fabricated using the BSF process are given in Figure 9, in which a shunted solar cell shows performance degradation by a reduction in Voc and maximum power available from the cell. During this period, work has progressed to analyze the shunting characteristics caused by the BSF process using ion microprobe/SIMS* and optical microscope examination.

1.0 JUNCTION SHUNTING BY THE BSF PROCESS

A large number of solar cells were investigated to find clues for the shunting problem using an optical microscope. Results indicated that shunted solar cells generally had surface contamination (front junction side) in the form of penetration pits and alloy patterns. The trend was the greater the number of contamination patterns, the higher the probability and degree of shunting. Figure 10 is shows photographs of contaminants at high magnification, in which the crystallographic orientation

*The analysis was carried out using CAMECA ims 3F by Charles Evans Associates (San Mateo, CA).

orientation dependence of contamination patterns is noticed; (a) for a (100) substrate and (b) for a (111) substrate. Ion microprobe/SIMS was used to identify the composition of the contaminants. Aluminum image formation by the probe strongly indicated that the contaminants were aluminum (Figure 10(c) is a photograph of the aluminum image). Mechanical lapping removed the surface patterns completely, which suggests that the contaminants are located at the front junction surface. Sputtering by the ion source (oxygen) also showed the same results; i.e., the pattern in (b) of Figure 10 has disappeared after about 2 μm of silicon was sputtered away (no aluminum image could be obtained after the sputtering).

The ion microprobe/SIMS was further utilized to check if surface areas, free from visual contaminants, were also contaminated. Thus, a surface profile analysis (front junction side) was performed for mass numbers up to 60 by the probe and a typical result is shown in Figure 11. The figure indicates high spikes in the ion intensity counts for elements such as B, C, O, Na, Al, K, Ca and some silicon complexes. The surface concentration of aluminum was calculated from the silicon counts, suggesting a concentration of $6x10^{18}$ atoms/cm^3 which is a concentration close to the solid solubility of aluminum (about $1x10^{19}$ atoms/cm^3) in silicon. The depth profile of aluminum was also obtained to see how deeply the aluminum penetrated into the bulk silicon, or towards the junction. Figure 12 is a result of the depth profile; mass numbers 14, 27, and 11 for silicon, aluminum and boron, respectively. The depth of aluminum penetration was estimated from the sputtering rate used to be around 500-1000 angstroms (the junction depth was about 3000 angstroms). Calculated concentrations are also indicated in Figure 12, showing initially high concentration of

aluminum close to surface (solid solubility limit down to about 300-400 angstroms), leveling off to a concentration of $4x10^{16}$ atoms/cm^3 at a depth of 1500 angstroms. A significant concentration of boron was also observed at the surface and was thought to have originated from the aluminum paste used for the BSF process. The boron concentration shows a similar profile to aluminum and tapers off at a concentration of about $4x10^{15}$ atoms/cm^3. This is equivalent to the boron concentration of the starting boron-doped p-type silicon of 1-3 ohm-cm resistivity.

Past experience indicated that junction shunting by the BSF process depends on the starting silicon properties, such as doping concentration (some results were reported in the Fourth Quarterly Report), crystallographic orientation or defects. Thus, work has progressed to see if there is a difference in aluminum diffusion as a function of crystallographic orientation; (111) versus (100). About 3000 angstroms of aluminum was evaporated on the wafers of starting resistivity around 10 ohm-cm and alloyed following the same procedure used for the paste BSF process. The samples were analyzed for luminum depth profile on the alloyed side by the microprobe. Note: This experiment was performed to save the probe operation time since depth profiling of the Al paste alloy layer takes a long time due to relatively deep penetration depth of aluminum. The results of the profiling are given in Figure 13; (a) for (100) orientation and (b) for (111) orientation. The aluminum penetration depth in (100) is larger than that of the (111) by approximately a factor of two. The same experiment was performed on dendritic webs which have (111) orientation and similar results were obtained as shown in (c) of Figure 13.

Since ion microprobe/SIMS analysis showed aluminum contamination near the front surface, work has progressed to protect the front surface by depositing various thickness of SiO_2 on the diffused surface before aluminum paste was applied. SiO_2 thickness of 0.5 μm, 1 μm, 1.5 μm and 2 μm were used. The test was carried out on 3" wafers carrying a pattern of 6-2x2 cm solar cells. Each wafer was finally cut to 2x2 cm solar cells for evaluation. The results indicated that, statistically, the number of shunted cells and the degree of shunting decreased as the thickness of the protective layer increased. To back-up this result another batch of solar cells was processed, showing a similar result. Ion microprobe analysis on these solar cells suggested that the penetration depth and the front surface concentration of aluminum show a tendency to decrease as the thickness of the protective layer increased.

2.0 *DISCUSSION ON BSF*

So far the ion probe has been used to find the origin of the junction shunting problems by analysis of the aluminum contamination on the front junction side. Now, the emphasis of this work has slightly shifted to check why the BSF process is so effective in improving solar cell performance, by analysis of aluminum (or other element used for BSF process such as boron) concentration profile on the back side of solar cell using the ion probe.

Aluminum depth profiling of the BSF, formed by an aluminum paste alloy process, were performed on CZ solar cells of (111) and (100) orientation and on dendritic web. The results are given in Figure 14 for CZ (100),

Figure 15 for CZ (111) and Figure 16 for dendritic web. The figures suggest;

(1) Aluminum penetration depth by the BSF process ranges between 1.5 and 4 μm,

(2) Solid solublity limit of aluminum almost extend to the end of the penetration front, and

(3) Aluminum concentration falls off drastically at the interface between silicon and the alloy layer, CZ (100) orientation shows a lesser degree of concentration change at the interface.

Note: These should be regarded as preliminary results since no tests on tests on reproducibility of the results have been done.

Depth profiles of other BSF processes utilizing boron sources on p-type starting substrates, either by boron nitride (BN) diffusion or boron ion-implantation, were performed using the ion microprobe. The results are shown in Figure 17 for the BN process and figure 18 for the implantation process, indicating;

(1) Boron penetration depths are about 4000 angstroms, which is relatively small compared with the aluminum paste process,

(2) Interface regions make rather smooth transistions compared with the BSF process using Al paste, and

(3) Boron concentration in the doped regions is considerably lower than the solid solubility of boron, which is about $1\text{-}3\times10^{20}$ atoms/cm^3 at room temperature.

Generally, the BSF, formed by either BN diffusion or boron ion-implantation, was less effective, specifically in terms of improvements in open circuit voltage, compared with the BSF from the Al paste alloy process. This could possibly be explained in terms of (1) penetration depth, the larger the better, (2) concentration profile at the interface, the more abrupt the better, and (3) concentration at the doped region, the higher the better i.e., the closer the solid solubility, the better. Further work is expected to extend these results.

FIGURE 9

TYPICAL ILLUMINATION CHARACTERISTICS OF TWO BSF PROCESS SOLAR CELLS; A GOOD CELL AND A SHUNTED CELL

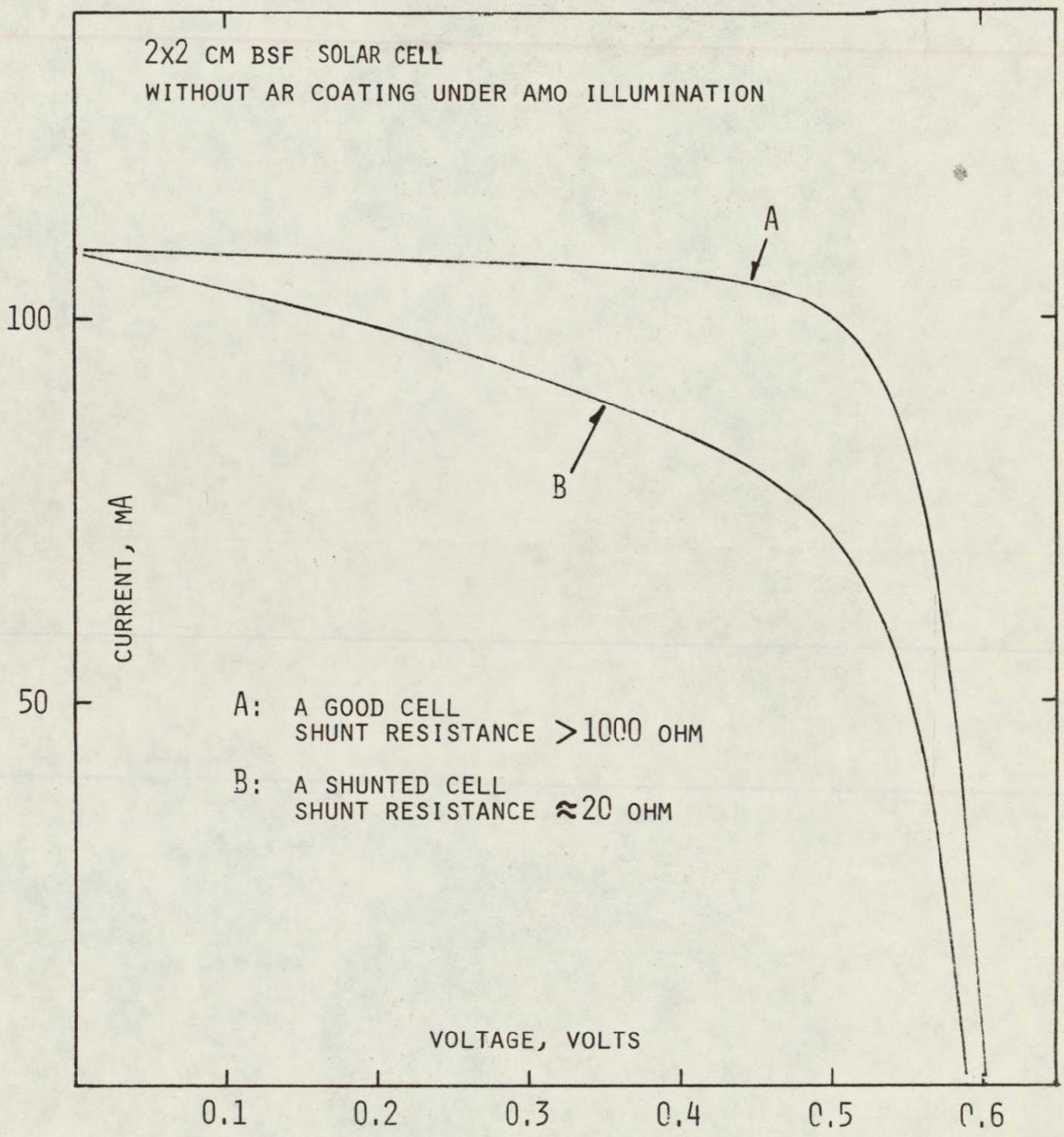

FIGURE 10

SURFACE CONTAMINATION CONTAMINANTS FROM THE BSF PROCESS

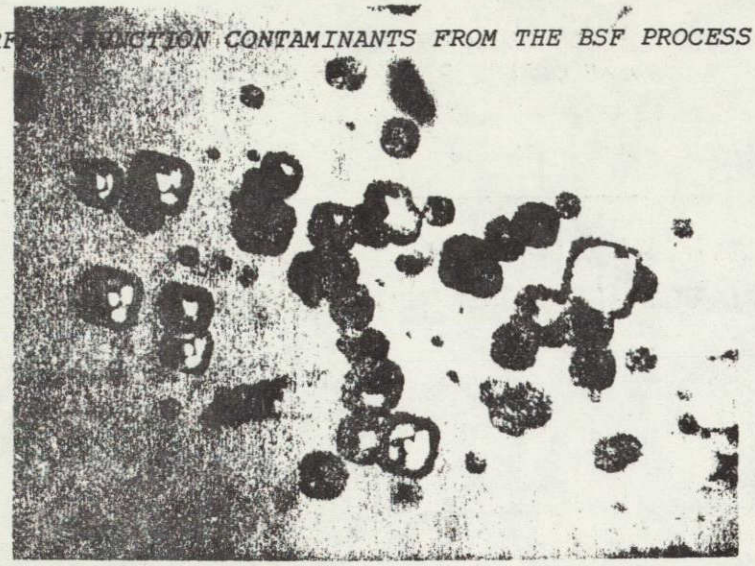

(A)

CONTAMINANTS ON (100) WAFER

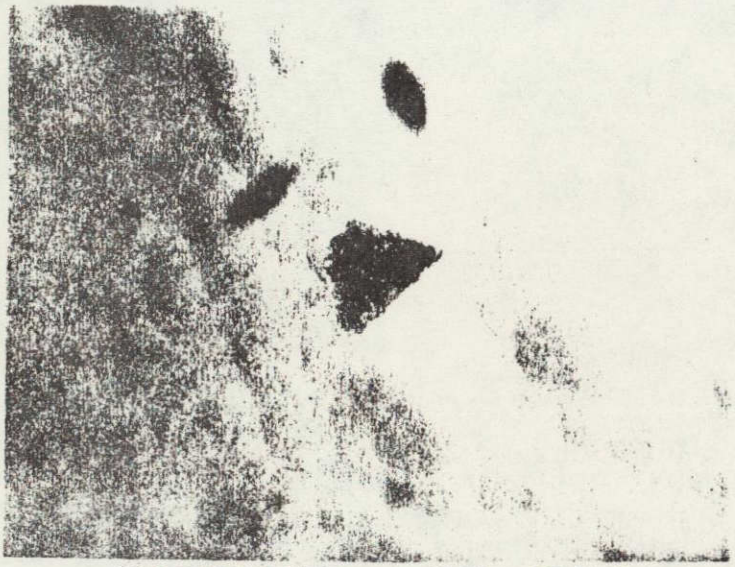

(B)

CONTAMINANTS ON (111) WAFER

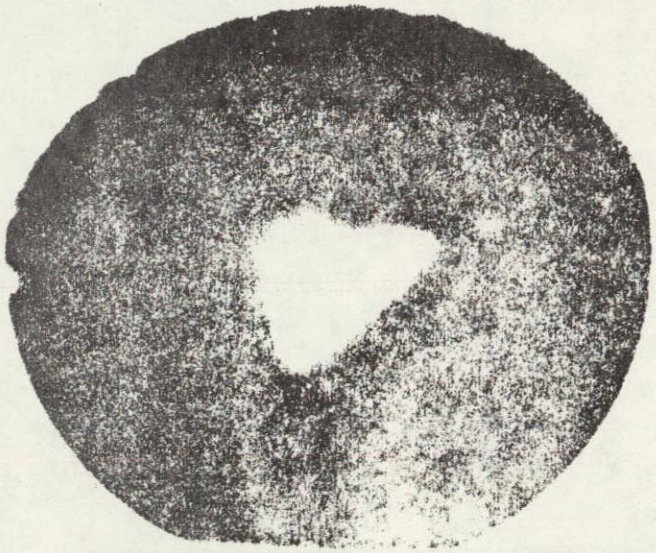

(C)

ALUMINUM IMAGE (BRIGHT TRIANGLE PATTERN)
BY ION MICROPROBE/SIMS

FIGURE 11

FRONT SURFACE ANALYSIS (SIMS, MASS SPECTRUM) OF A SOLAR CELL FROM THE BSF PROCESS

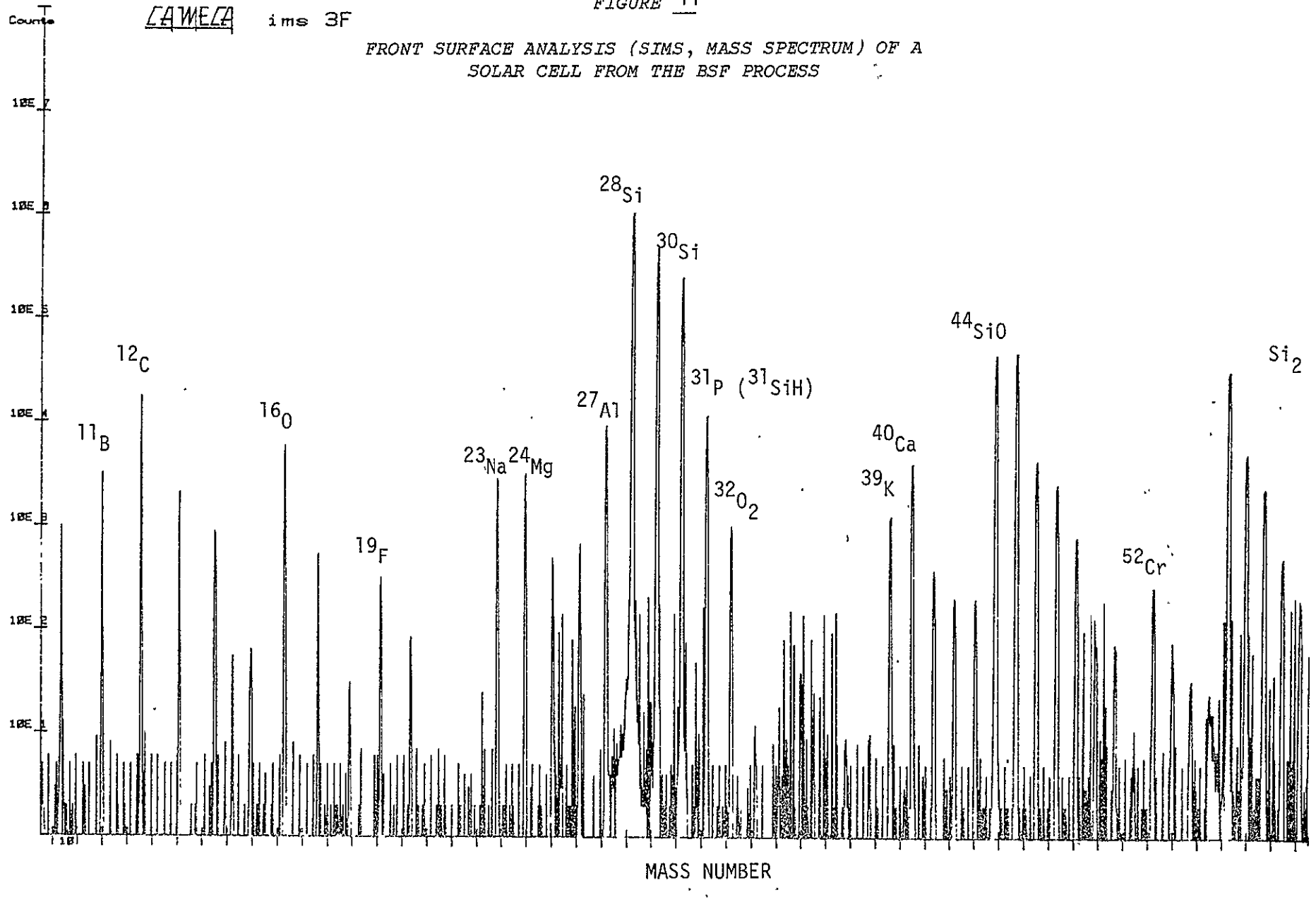

FIGURE 12

DEPTH PROFILE OF ALUMINUM (MASS NUMBER 27) BY ION MICROPROBE/SIMS

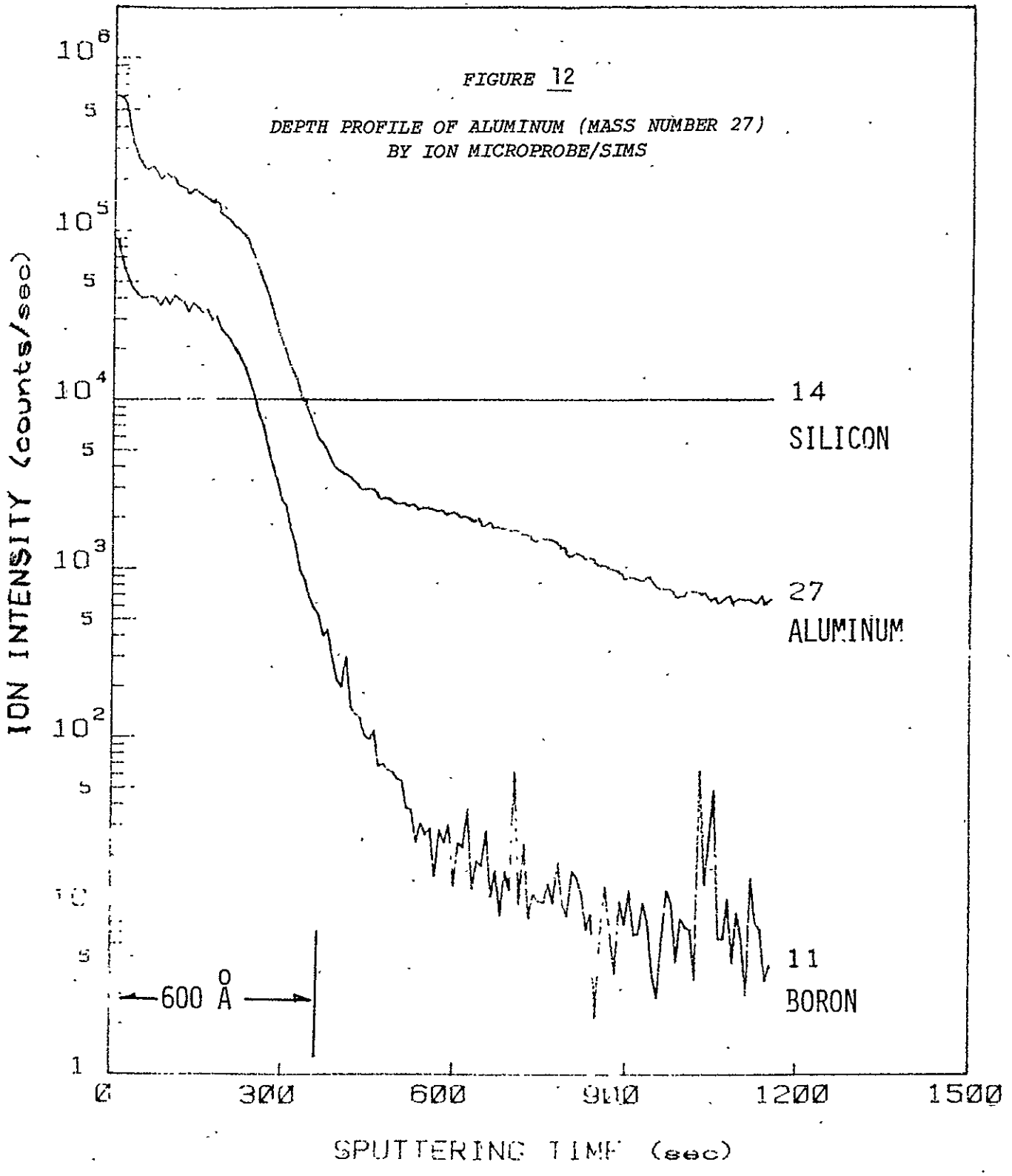

FIGURE 13a

ALUMINUM PENETRATION PROFILE (SIMS) ON

(a) A CZ (100) Wafer

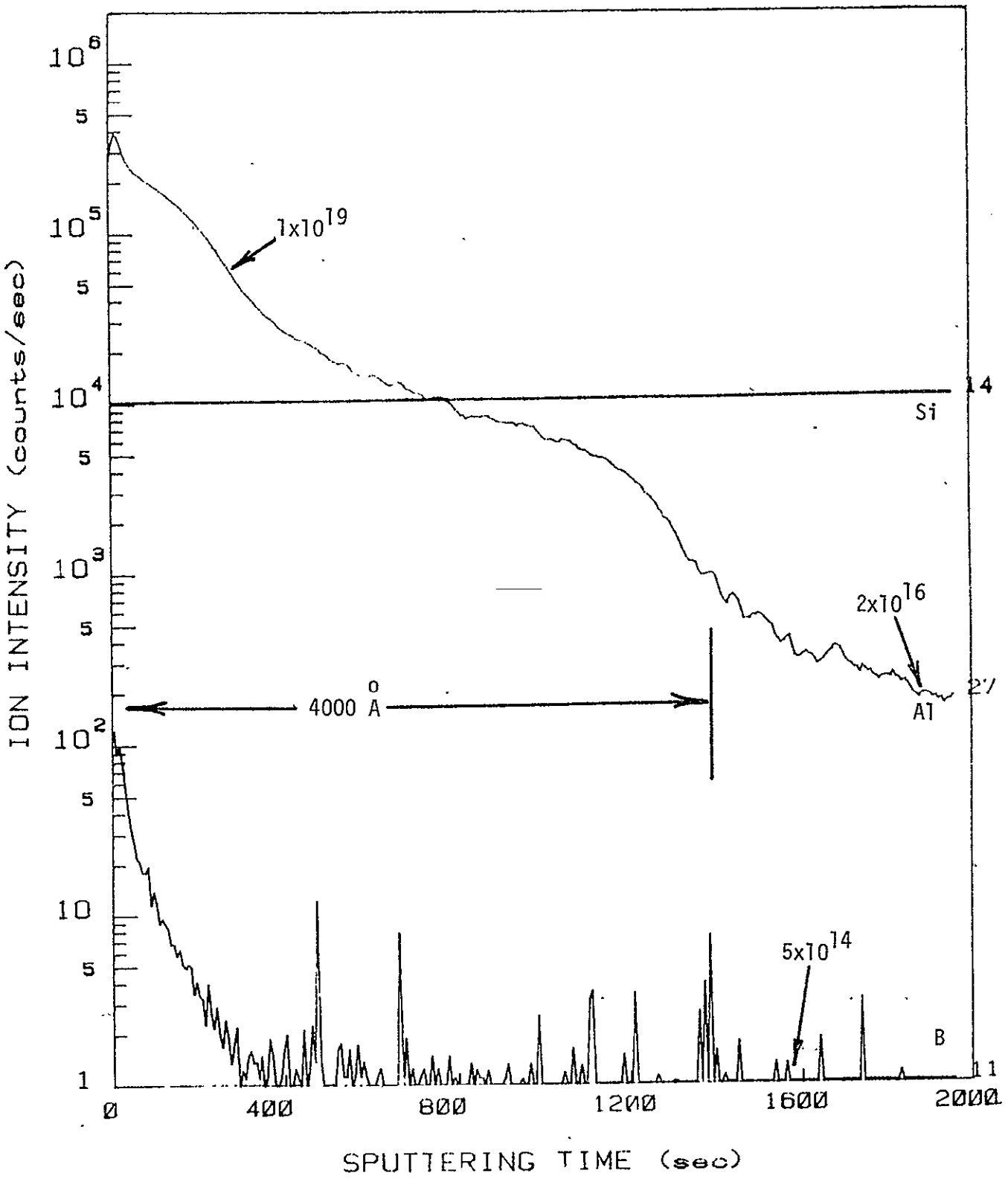

FIGURE 13b

ALUMINUM PENETRATION PROFILE (SIMS) ON

(b) A CZ (111) Wafer

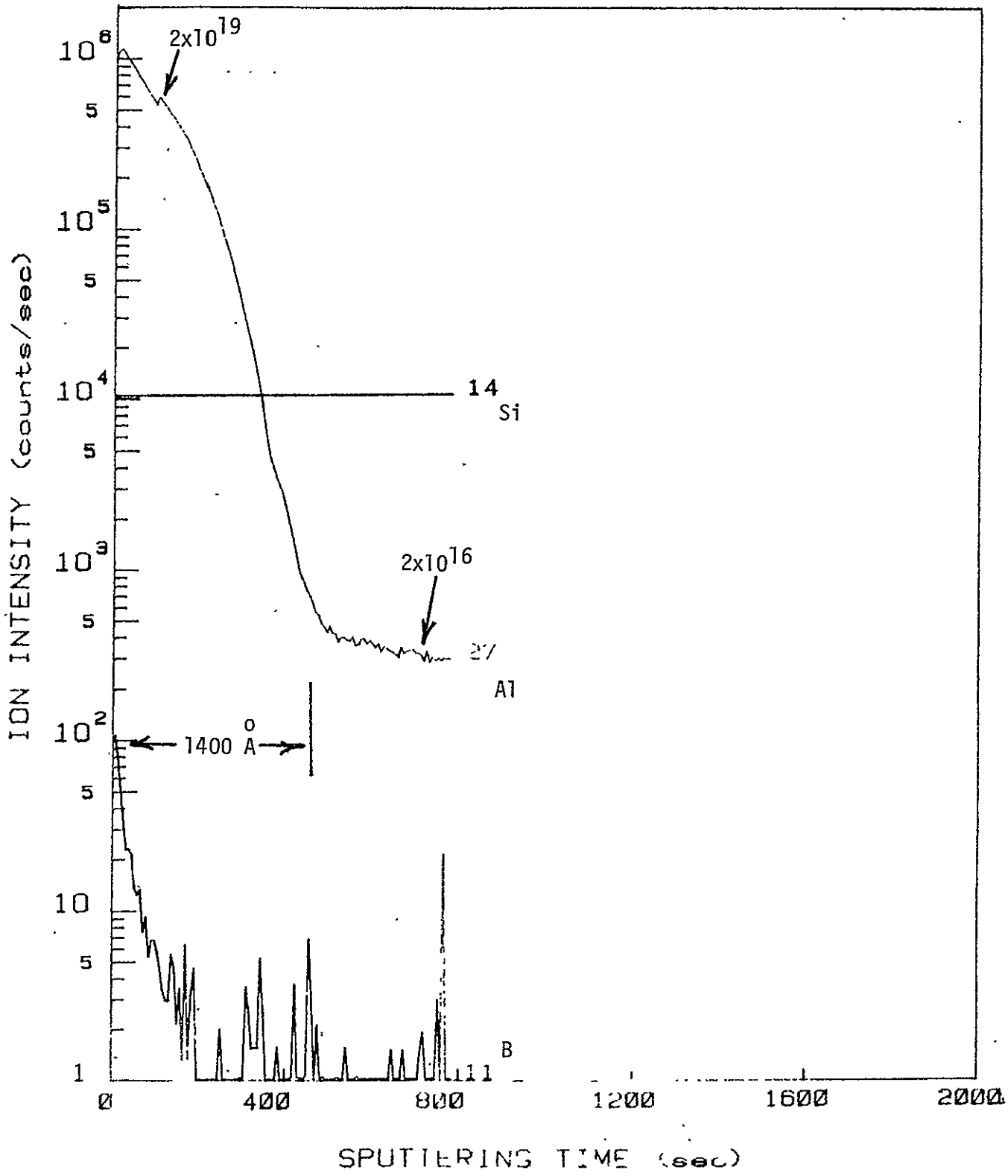

FIGURE 13c

ALUMINUM PENETRATION PROFILE (SIMS) ON

(c) A Dendritic Web

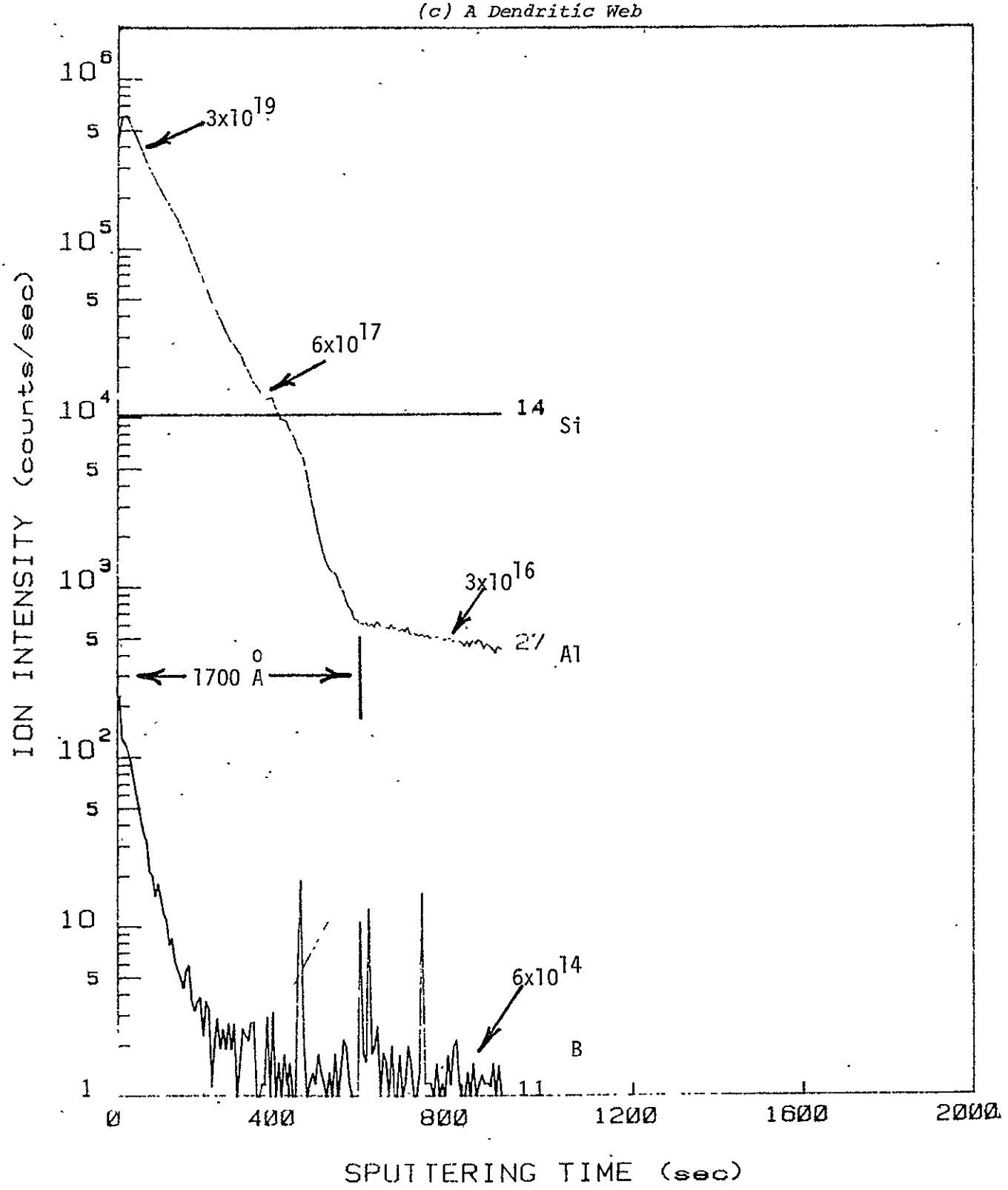

FIGURE 14

ALUMINUM DEPTH PROFILE (SIMS) OF THE BSF APPLIED ON A CZ (100) WAFER

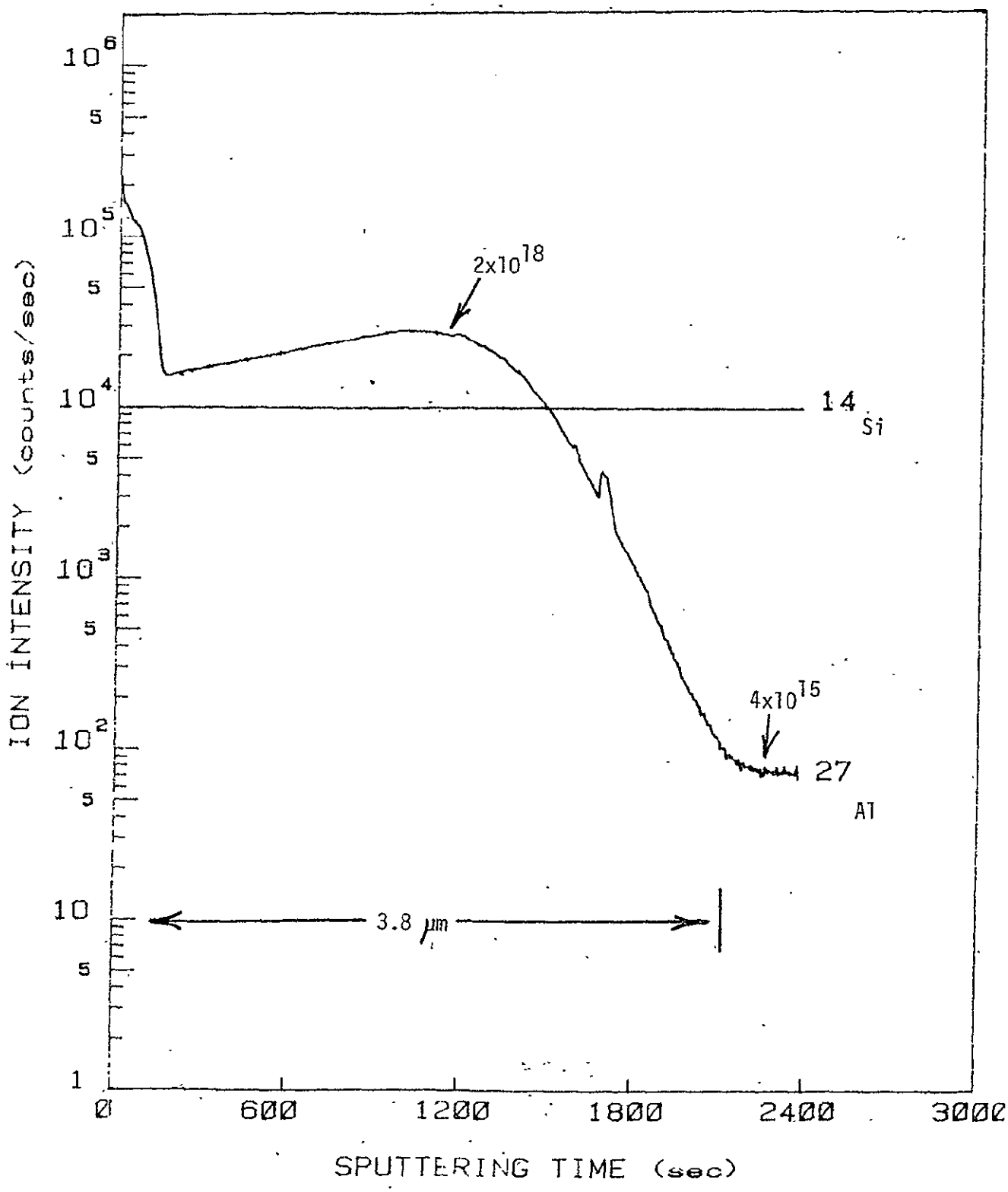

FIGURE 15

ALUMINUM DEPTH PROFILE (SIMS) OF THE BSF APPLIED ON A CZ (111) WAFER

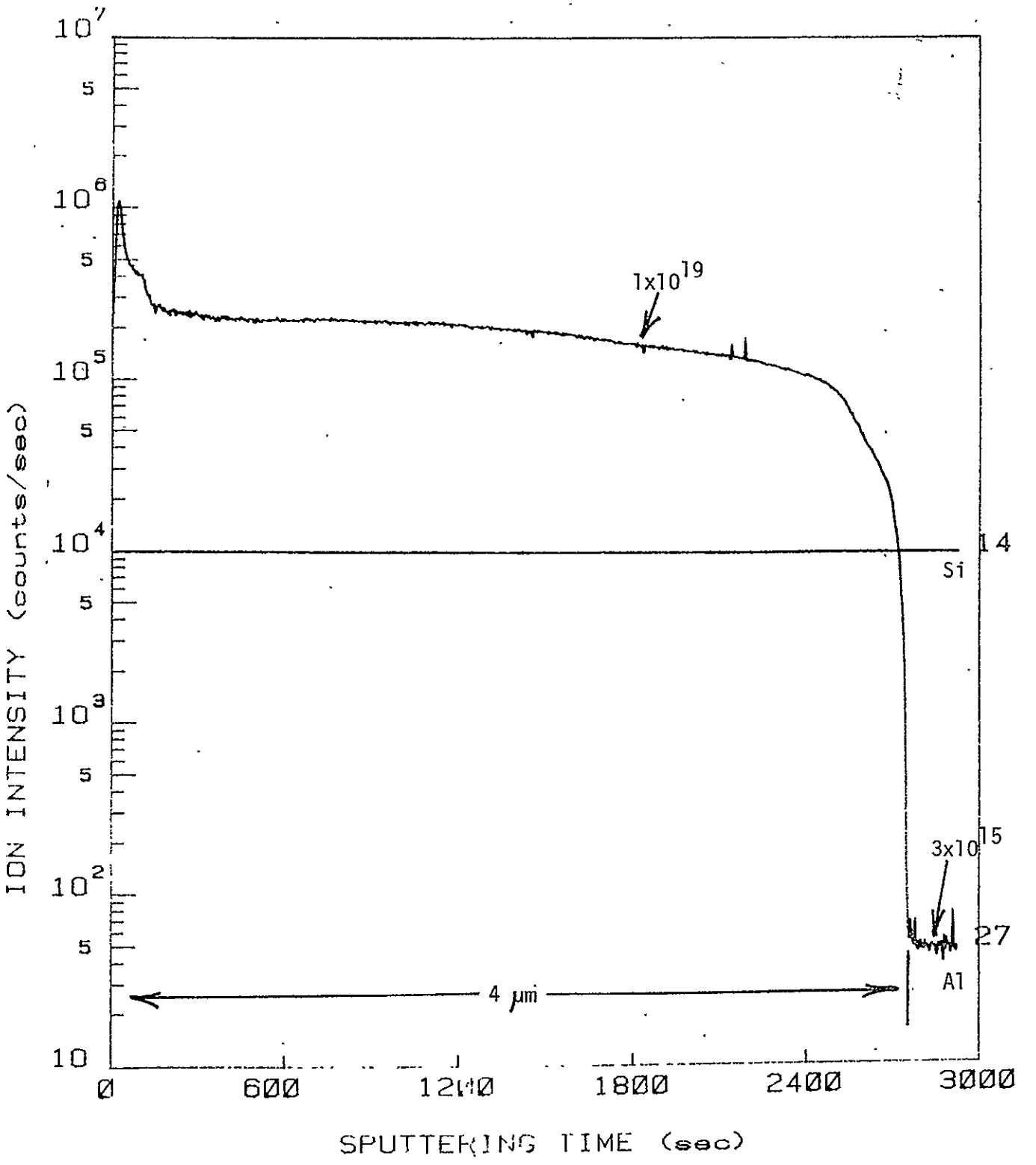

FIGURE 16

ALUMINUM DEPTH PROFILE (SIMS) OF THE BSF APPLIED ON A DENDRITIC WEB

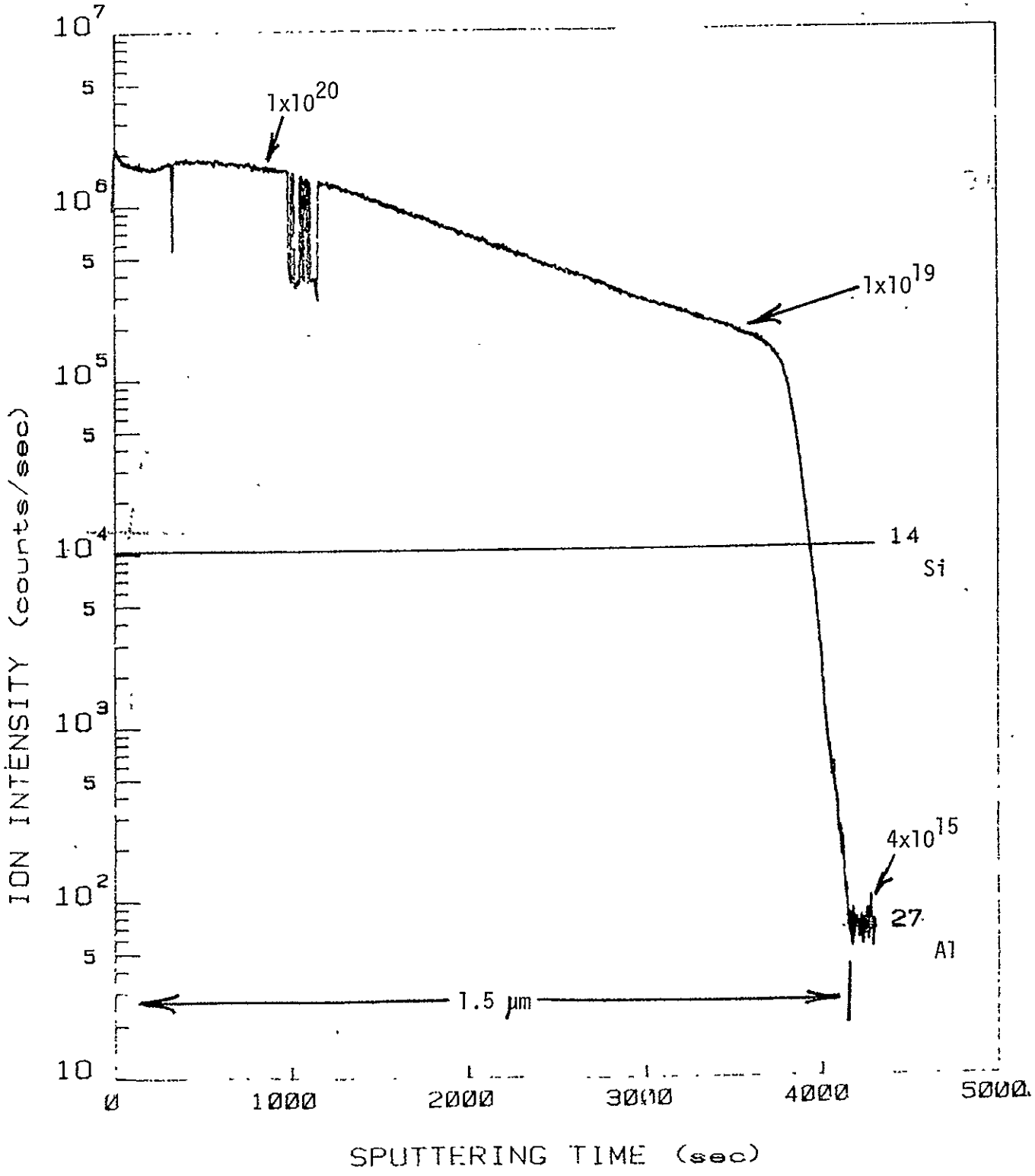

FIGURE 17

BORON DEPTH PROFILE (SIMS) OF THE BSF APPLIED BY BORON NITRIDE DIFFUSION ON CZ SILICON

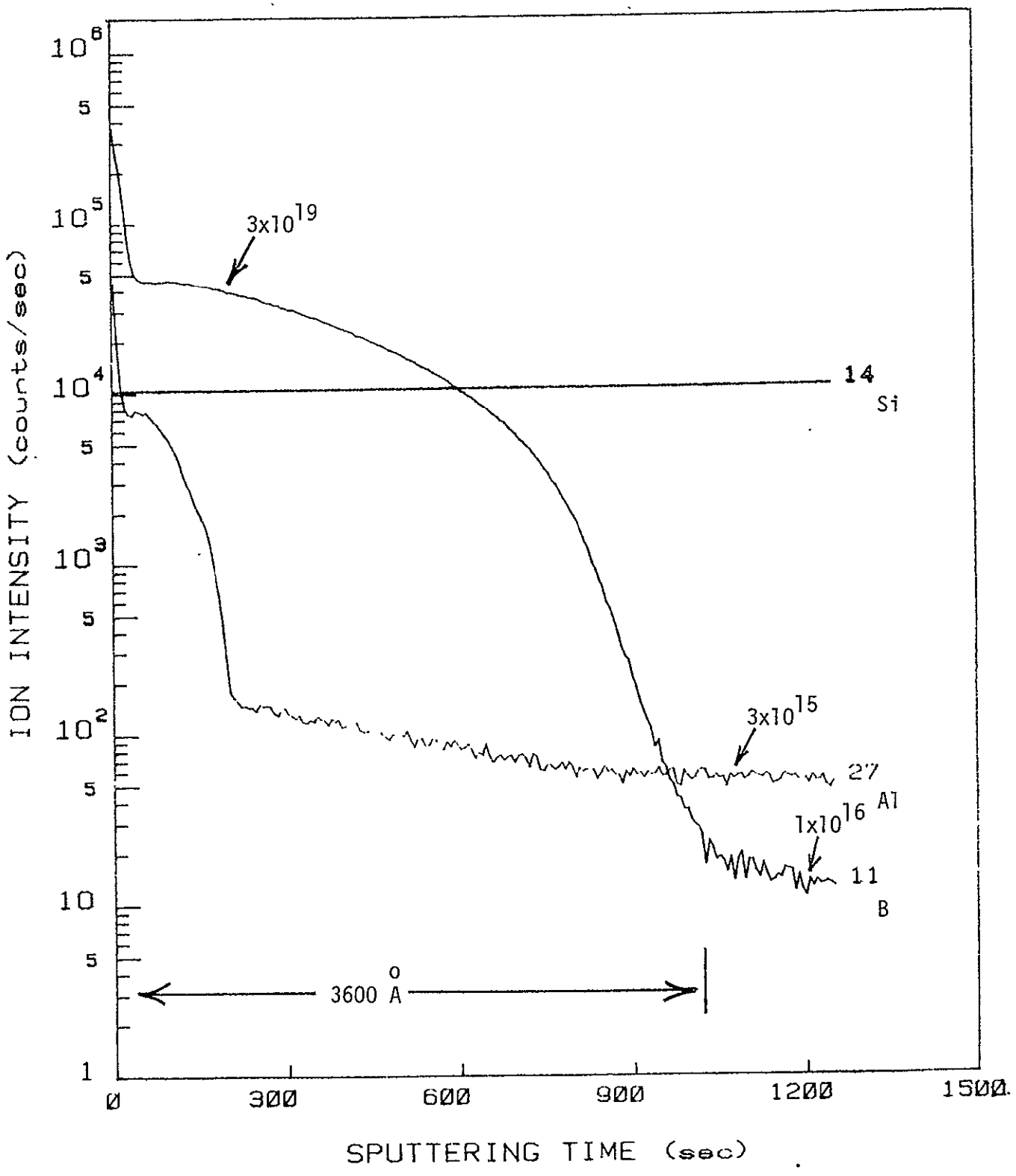

FIGURE 18

BORON DEPTH PROFILE (SIMS) OF THE BSF APPLIED BY ION IMPLANTATION ON A CZ SILICON

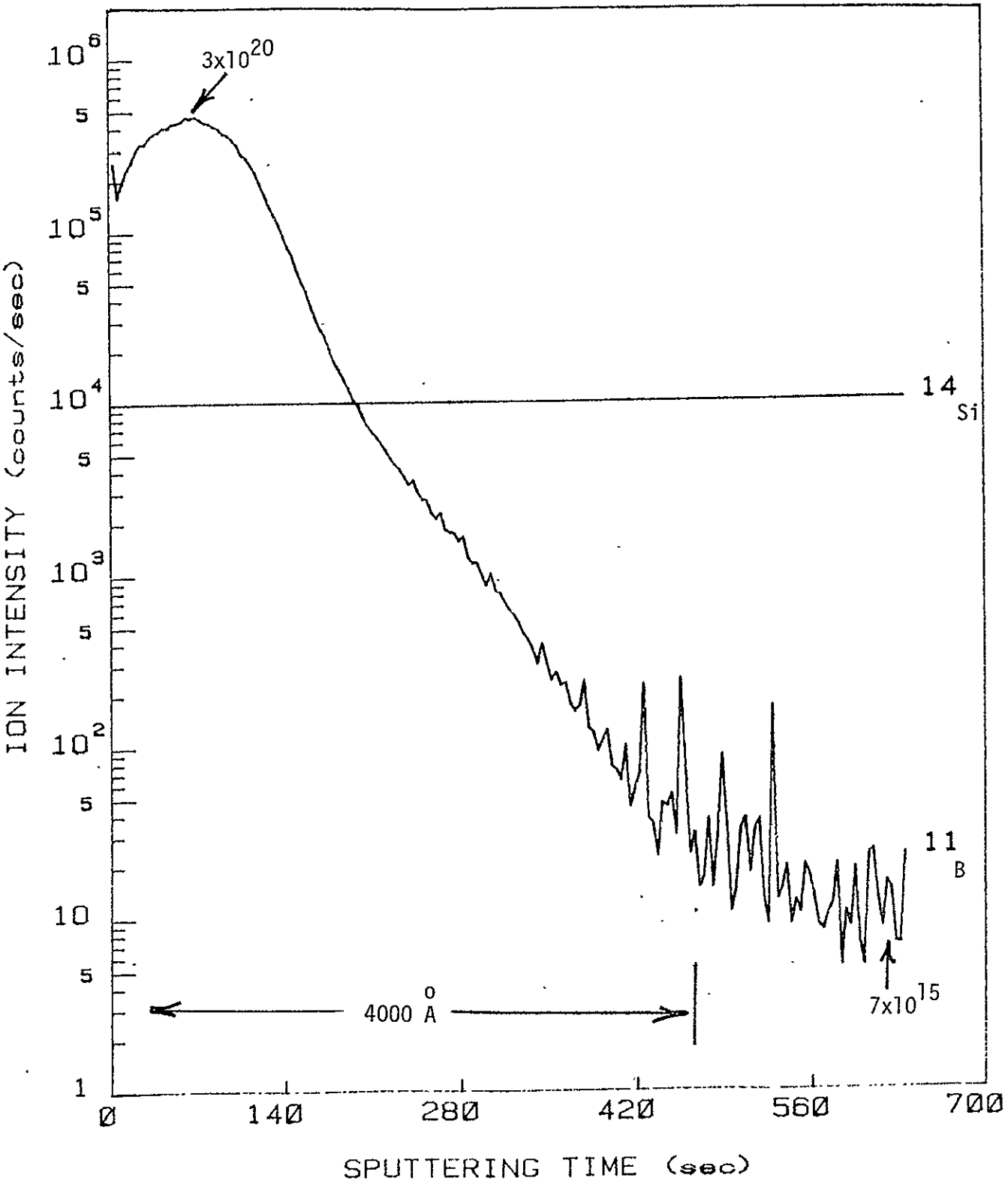

III. CONCLUSIONS AND RECOMMENDATIONS

Overall, the conclusions for this reporting period are similar to those made previously, namely:

- *The baseline process serves as a useful evaluation method, and the various measurements made show good internal consistency and repeatability.*

- *Analysis of the baseline process results allows identification of possible processing areas which will increase cell output. The processes which can give the most improvement are chosen to offset the most serious deficiencies noted after the standard processing.*

- *Good examples of such "custom-improvement" are the success of grain boundary passivation for EFG ribbon, and inclusion of a back surface field for dendritic web.*

- *The continued study of the detailed interaction of sheet silicon properties, and various process steps and sequences, is useful both for estimates of the highest efficiency obtainable from the sheet-cells, and also for guiding attention to possible sensitive areas when low cost process steps are applied to the various sheet forms.*

- *The studies of the shunting effects observed when the BSF process is used are timely because several other groups have reported similar problems, and it is important to have a non-interfering method so that*

the correlation of the BSF process with the increase obtained for the various sheet forms can be clearly identified.

- *The inclusion of AM1 measurements as well as AM0 is adding useful information to the JPL program.*

These conclusions lead to the recommendation that the work continue along the same lines, and that the results be rapidly fedback (via JPL) to the sheet manufacturers, to allow consideration of the results obtained while improved growth methods are being developed.

IV. WORK PLAN STATUS

The following silicon sheet materials are expected to be processed and evaluated during the next period.

- *Cast Silicon by HEM (Crystal Systems)*
- *Silicon on Ceramic (SOC, Honeywell)*
- *Semi-continuous CZ Ingots by the HAMCO Process*

Work will continue to identify mechanisms leading to junction shunting problems by the BSF process.

V. REFERENCES

(1) H.I. Yoo, et.al., "Silicon Solar Cell Process Development, Fabrication and Analysis", JPL Contract No. 955089, Fourth Quarterly Report, September, 1979.

(2) H.I. Yoo, et.al., "Silicon Solar Cell Process Development, Fabrication and Analysis", JPL Contract No. 955089, Annual Report, June, 1979.

APPENDIX I

TIME SCHEDULE

APPLIED SOLAR ENERGY CORPORATION
formerly Optical Coating Laboratory Photoelectronics Division
15251 E Don Julian Road P.O. Box 1212
City of Industry, California 91746
(213) 968-6581 Twx 910-584-4890

TIME SCHEDULE (PHASE II)

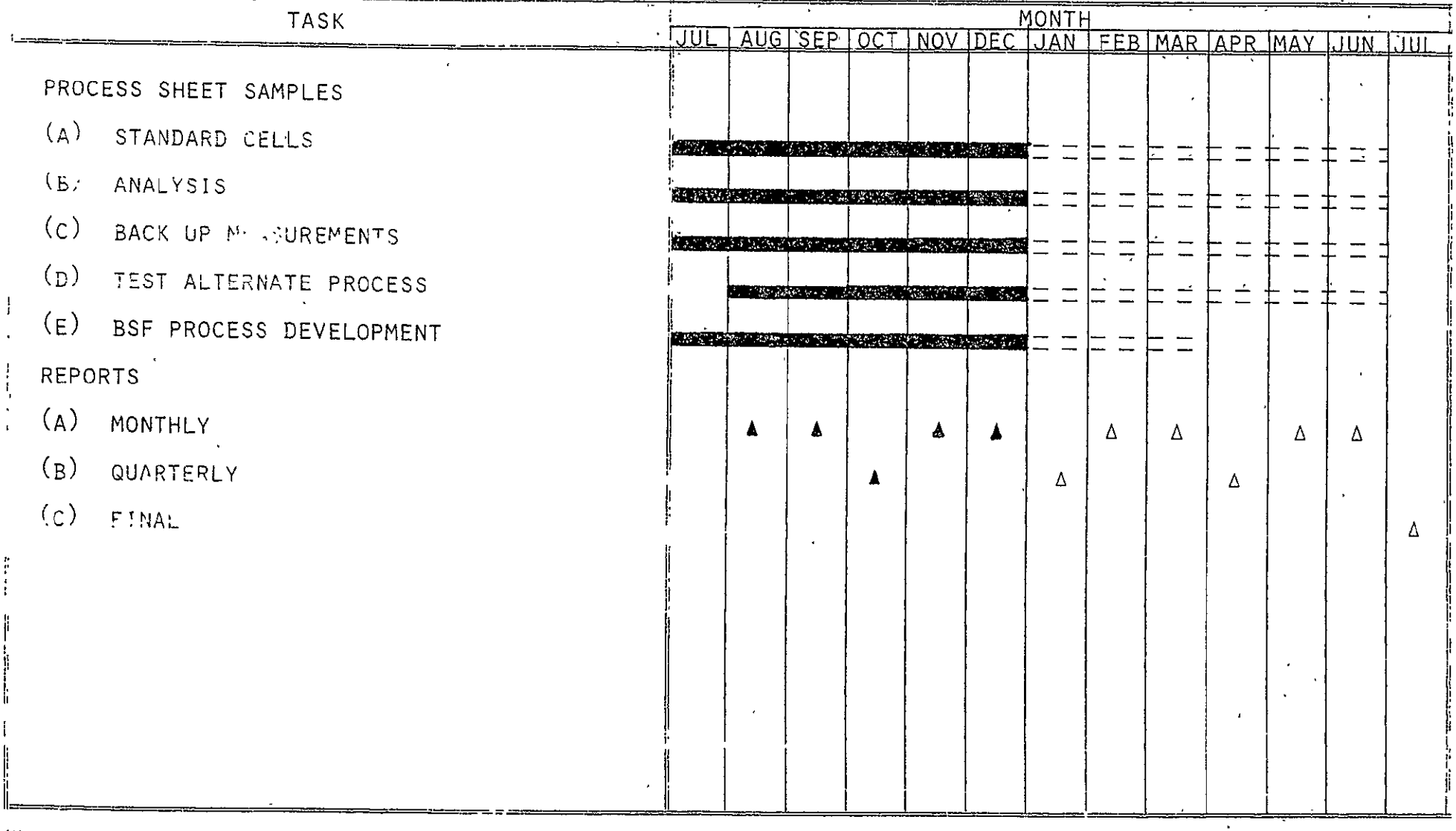

APPENDIX II

ABBREVIATIONS

ABBREVIATIONS

V_{OC}: *Open Circuit Voltage*

I_{SC}: *Short Circuit Current*

J_{SC}: *Short Circuit Current Density*

I_{SCR}: *Short Circuit Current (Red Response) at Wavelength Above* $\sim .6\ \mu m$

I_{SCB}: *Short Circuit Current (Blue Response) at Wavelength Below* $\sim .6\ \mu m$

CFF: Curve Fill Factor

η : *Solar Cell Conversion Efficiency*

L: Minority Carrier Diffusion Length (D.L.)

I_{MAX}: *Current at Maximum Power Point*

V_{MAX}: *Voltage at Maximum Power Point*

P_{MAX}: *Maximum Power Point*

BSF: Back Surface Field

BSR: Back Surface Reflector

V_B: *Bias Voltage*

I_o: *Diode Saturation Current*

HEM: Heat Exchanger Method

EFG: Edge Defined Film-Fed Growth

SOC: Silicon on Ceramic

RTR: Ribbon-to-Ribbon

SPV: Surface Photòvoltage

MLAR: Multi-Layer Anti-Reflective

R_s: *Series Resistance*

APPENDIX III

ELECTRICAL DATA SHEETS FOR SOLAR CELLS FROM MULTI-RIBBON EFG (RH)

SOLAR CELL ELECTRICAL DATA

CELL DESCRIPTION: EFG (RH) Solar Cells, ~2x2 cm, Surface Etching #1, STD Process
SiO AR Coating

TEST CONDITION: AMO

TEMPERATURE: 25°C Test Block DATE:

NO.	V_{OC}	I_{SC}	I_{SCB}	I_{SCR}	I_{Max}	V_{Max}	P_{Max}	CFF	η	AREA
	mV	mA	mA	mA	mA	mV	mW	%	%	cm^2
1.	520	96	44	51	82	412	33.78	67.7	6.3	3.96
2	504	87		broken during Measurement						
3	505	98	43	53	72	395	28.44	57.5	5.4	3.87
4	524	104	46	56	88	393	34.58	63.5	6.5	3.96
5	538	100	44	55	81	415	33.62	62.4	6.4	3.89
6	507	100	43	55	76	400	30.40	59.9	5.8	3.87
		EFG controls (EFG cells without surface etching)								
7	496	95	42	50	81	385	31.19	67.5	5.8	3.96
8	502	90	41	47	80	410	32.80	72.6	6.2	"
9	511	95	43	50	87	410	35.67	73.5	7.0	3.78
10	495	97	44	52	78	405	31.59	65.8	5.9	3.95
*	EFG Solar cell Identification									
	Cell # 1, 2, 3, 7, 8 from EFG Ribbon JPL I.D 5-1092 section 817									
	Cell # 4, 5, 6, 9, 10 from " " " " 4 120									

SJ

SOLAR CELL ELECTRICAL DATA

CELL DESCRIPTION: EFG (RH) Solar Cells, ~2x2 cm, Surface Etching #2, STD Process
SiO AR Coating

TEST CONDITION: AMO

TEMPERATURE: 25°C Test Block DATE:

NO.	V_{OC} mV	I_{SC} mA	I_{SCB} mA	I_{SCR} mA	I_{Max} mA	V_{Max} mV	P_{Max} mW	CFF %	η %	AREA cm^2
1	525	90	42	46	82	399	32.7	69	6.2	3.92
2	510	88	41	45	73	389	28.4	63	5.4	3.91
3	502	78	38	37	71	389	27.6	71	5.2	4
4	506	78	38	38	72	394	28.4	72	5.3	3.94
5	516	89	41	46	82	409	33.5	73	6.3	3.91
6	502	80	39	38	72	394	28.4	71	5.3	3.95
		EFG control cells (EFG cells without surface etching)								
7	502	81	40	39	72	389	28.0	69	5.3	3.94
8	526	93	43	48	79	404	31.9	65	6.0	3.92
		Single crystal CZ control cells								
C-1	591	129	50	80	114	479	54.6	72	10.3	3.93
C-2	584	122	47	75	105	474	49.7	70	10.0	3.67
C-3	593	131	51	81	120	461	55.3	71	10.4	3.92
-X-	EFG	Solar cell	Identification.							
	All	cells, from cell # 1 to 8, from				EFG Ribbon JPL I.D 5-1095 Section 63				

SOLAR CELL ELECTRICAL DATA

CELL DESCRIPTION: EFG (RH) Solar Cells, ~2x2 cm, Surface Texturizing, STD Process
SiO AR Coating

TEST CONDITION: AMO

TEMPERATURE: 25°C Test Block DATE:

NO.	V_{OC}	I_{SC}	I_{SCB}	I_{SCR}	I_{Max}	V_{Max}	P_{Max}	CFF	n	AREA
	mV	mA	mA	mA	mA	mV	mW	%	%	cm^2
1	524	89	42	46	80	410	32.8	70	6.2	3.93
2	516	85	40	43	76	412	31.3	71	5.9	"
3	465	82	37	42		shunted	badly			
4	516	84	39	43	75	405	30.4	70	5.7	3.93
		EFG control cells (EFG cells without texturizing)								
5	506	77	37	38	63	410	25.8	66	5.1	3.72
6	513	83	40	41	76	403	30.6	72	5.8	3.94
7	517	86	40	44	76	403	30.6	69	5.8	3.92
*	EFG Solar cell Identification									
	Cell #	1, 5, 6, 7		from	EFG Ribbon JPL I.D 5-1095 section 175					
	Cell #	2, 3		"	"	"		"	" 225	
	Cell #	4		"	"	"		"	" 265	

SOLAR CELL ELECTRICAL DATA

CELL DESCRIPTION: EFG (RH) Solar Cells, 2x2 cm, BSF Process
SiO AR Coating

TEST CONDITION: AMO

TEMPERATURE: 25°C Test Block DATE:

NO.	V_{OC}	I_{SC}	I_{SCB}	I_{SCR}	I_{Max}	V_{Max}	P_{Max}	CFF	η	AREA
	mV	mA	mA	mA	mA	mV	mW	%	%	cm^2
1	533	105	49	54	93	432	40.18	72	7.4	4
2	533	104	49	53	93	432	40.18	73	7.4	"
3	498	106	47	57		Shunted				"
4	540	107	49	56	96	445	42.72	74	7.9	"
5	520	103	47	54	79	410	32.39	61	6.0	"
6	520	105	49	54		Shunted				"
7	539	109	50	56	97	440	42.68	73	7.9	"
8	519	101	49	50	84	406	34.10	65	6.3	"
9	540	109	50	57	96	435	41.76	71	7.7	"
10	532	103	48	53	91	431	39.22	72	7.3	"
11	454	101	48	51		Shunted				"
12	514	106	48	56		"				"
13	491	99	48	49		"				"
14	530	99	46	51	89	434	38.63	74	7.2	"
15	534	106	50	56	96	435	41.76	74	7.7	"
*	All EFG Solar cells from EFG Ribbon					JPL I.D 5-1095				

↺

SOLAR CELL ELECTRICAL DATA

CELL DESCRIPTION: EFG (RH) Solar Cells, ~2x2 cm, Grain Boundary Passivation, STD Process
SiO AR Coating

TEST CONDITION: AMO

TEMPERATURE: 25°C Test Block DATE:

NO.	V_{OC}	I_{SC}	I_{SCB}	I_{SCR}	I_{Max}	V_{Max}	P_{Max}	CFF	η	AREA
	mV	mA	mA	mA	mA	mV	mW	%	%	cm^2
1	543	105	48	56	100	427	42.7	75	7.9	4.00
2	524	101	47	53	93	427	39.7	75	7.4	"
3	516	92	43	48	78	414	32.3	68	6.2	3.87
4	550	109	49	60	101	444	44.8	75	8.2	4.00
5	536	94	44	48	87	419	36.5	72	7.1	3.81
6	550	103	46	56	94	439	41.3	73	8.2	3.71
*	EFG Solar Cells Identification									
	Cell # 1	from EFG Ribbon JPL I.D 5-1095						section	63	
	Cell # 2, 3	"	"			"	"	"	143	
	Cell # 4, 5, 6	"	"			"	"	"	175	

SOLAR CELL ELECTRICAL DATA

CELL DESCRIPTION: EFG (RH) Solar Cells, ~2x2 cm, Gettering by Diffusion Glass, STD Process
SiO AR Coating

TEST CONDITION: AMO

TEMPERATURE: 25°C Test Block DATE:

NO.	V_{OC} mV	I_{SC} mA	I_{SCB} mA	I_{SCR} mA	I_{Max} mA	V_{Max} mV	P_{Max} mW	CFF %	n %	AREA cm^2
1	501	83	41	40	75	395	29.63	71.2	5.5	3.95
2	506	90	42	46	82	405	33.21	73.9	6.2	3.96
3	487	88	41	45	69	365	25.19	58.8	4.7	3.93
4	504	90	43	45	80	400	32.00	70.6	6.0	3.95
5	503	88	42	45	79	395	31.21	70.5	5.8	3.95
6	516	92	44	47	81	415	33.62	70.8	6.3	3.95
		EFG Control Cells (EFG cells without gettering)								
7	496	95	42	50	81	385	31.19	67.5	5.8	3.96
8	502	90	41	47	80	410	32.80	72.6	6.2	"
9	511	95	43	50	87	410	35.67	73.5	7.0	3.78
10	495	917	44	52	78	405	31.59	65.8	5.9	3.95
*	EFG Solar cell Identification									
	Cell # 1, 2, 3, 7, 8		from EFG Ribbon JPL I.D 5-1092 section 87							
	Cell # 4, 5, 6, 9, 10		"	"	"	"	"	"	120	

59

APPENDIX IV

ELECTRICAL DATA SHEETS FOR SOLAR CELLS FROM DENDRITIC WEBS

SOLAR CELL ELECTRICAL DATA

CELL DESCRIPTION: Dendritic Web Solar Cells,~1"x1", BSF Process
MLAR Coating

TEST CONDITION: AMO

TEMPERATURE: 25°C Test Block DATE:

NO.	V_{OC} mV	I_{SC} mA	I_{SCB} mA	I_{SCR} mA	I_{Max} mA	V_{Max} mV	P_{Max} mW	CFF %	n %	AREA cm^2
1	588	244	97	146	227	485	110.1	76.7	12.6	6.45
2	580	242	97	146	220	470	103.4	73.7	11.9	"
3	585	242	97	145	220	470	103.4	73.0	11.9	"
4	560	229	94	134	209	450	94.1	73.3	10.8	"
5	559	232	95	136	207	445	92.1	71.0	10.6	"
6	559	150	61	88	141	425	59.9	71.5	10.7	4.15
7	520	212	95	117	192	427	82.0	74.4	9.4	6.45
		Single crystal Control cells (10 ohm-cm) with BSF								
CB-1	588	244	97	146	227	485	110.1	76.7	12.6	6.45
" -2	580	242	97	146	220	470	103.4	73.7	11.9	"
" -3	585	242	97	145	220	470	103.4	73.0	11.9	"
		Single crystal Control Cells (10 ohm-cm) without BSF								
C-1	558	238	93	145	202	450	90.9	68.5	10.4	6.45
C-2	560	237	93	144	226	412	93.1	70.2	10.7	"
*	Solar cell Identification.									
	Cell #	1, 2, 3	from	Web	JPL I.D	17-1099				
	Cell #	4, 5, 6	"	"	"	17-1107				
	Cell #	7	"	"	"	17-1117				

6

SOLAR CELL ELECTRICAL DATA

CELL DESCRIPTION: Dendritic Web Solar Cells, ~1"x1", BSF Process
MLAR Coating. Selected Cells for AM1 Measurement.

TEST CONDITION: AM1

TEMPERATURE: 25°C Test Block DATE:

NO.	V_{OC}	I_{SC}	I_{SCB}	I_{SCR}	I_{Max}	V_{Max}	P_{Max}	CFF	n	AREA
	mV	mA	mA	mA	mA	mV	mW	%	%	cm^2
1	583	200			187	485	90.7	78	14.1	6.45
5	555	187			173	460	79.6	77	12.3	"
		Single crystal control (10 ohm-cm) with BSF								
CB-1	586	199			185	485	89.7	77	13.9	6.45
CB-2	586	198			178	496	88.3	76	13.7	"
*	Solar cell Identification									
	Cell # 1	from Web			JPL I.D	17-1099				
	Cell # 5	"			" "	17-1107				

SOLAR CELL ELECTRICAL DATA

CELL DESCRIPTION: Dendritic Web Solar Cells, 2x2 cm, BSF + BSR Process
MLAR Coating

TEST CONDITION: AMO

TEMPERATURE: 25°C Test Block DATE:

NO.	V_{OC} mV	I_{SC} mA	I_{SCB} mA	I_{SCR} mA	I_{Max} mA	V_{Max} mV	P_{Max} mW	CFF %	η %	AREA cm^2
1	598	164	68	96	142	500	71.0	72.4	13.1	4
2	592	161	67	94	146	495	72.3	75.8	13.4	"
3	577	154	66	87	137	475	65.1	73.2	12.1	"
4	583	157	66	89	143	485	69.4	75.8	12.8	"
5	581	156	66	89	143	485	69.4	76.5	12.8	"
6	569	151	66	85	140	480	67.2	78.2	12.4	"
7	589	159	67	91	142	500	71.0	75.8	13.1	"
8	573	156	66	89	132	475	62.7	70.1	11.6	"
9	584	158	67	91	143	485	69.4	75.2	12.8	"
10	604	159	66	94	148	505	74.5	77.6	14.2	3.89
*	Solar cell Identification									
	Solar cell # 1		from	Web	JPL ID	17-1098				
	"	# 2	"	"	" "	17-1102				
	"	# 3	"	"	" "	17-1106				
	"	# 4, 5	"	"	" "	17-1112				
	"	# 6	"	"	" "	17-1113				
	"	# 7, 8, 9	"	"	" "	17-1153				

SOLAR CELL ELECTRICAL DATA

CELL DESCRIPTION: Dendritic Web Solar Cells, 2x2 cm, BSF + BSR Process
MLAR Coating. Cells for AM1 Measurement

TEST CONDITION: AM1
TEMPERATURE: 25°C Test Block DATE:

NO.	V_{OC}	I_{SC}	I_{SCB}	I_{SCR}	I_{Max}	V_{Max}	P_{Max}	CFF	η	AREA
	mV	mA	mA	mA	mA	mV	mW	%	%	cm^2
1	583	137			118	487	57.47	72	14.4	4
2	579	134			122	484	59.05	76	14.8	"
3	562	128			114	460	52.44	73	13.1	"
4	569	131			120	470	56.40	76	14.1	"
5	568	130			120	470	56.40	76	14.1	"
6	556	127			118	465	54.87	78	13.7	"
7	574	133			120	478	57.36	75	14.3	"
8	559	130			110	460	50.60	70	12.7	"
9	570	132			120	468	56.16	75	14.0	"
10	590	133			122	493	60.15	77	15.5	3.89

APPENDIX V

ELECTRICAL DATA SHEETS FOR SOLAR CELLS FROM HEM

SOLAR CELL ELECTRICAL DATA

CELL DESCRIPTION: HEM Solar Cells (Single Crystal), 2x2 cm, STD Process
SiO AR Coating. First of Two Sheets

TEST CONDITION: AMO

TEMPERATURE: 25°C Test Block DATE:

NO.	V_{OC}	I_{SC}	I_{SCB}	I_{SCR}	I_{Max}	V_{Max}	P_{Max}	CFF	n	AREA
	mV	mA	mA	mA	mA	mV	mW	%	%	cm^2
1	585	117	45	72	105	488	51.24	75	9.5	4
2	577	118	44	74	86	475	40.85	60	7.6	"
3	579	118	46	72	92	480	44.16	65	8.2	"
4	580	115	45	70	101	480	48.48	73	9.0	"
5	576	113	44	68	102	482	49.16	76	9.1	"
6	578	114	45	69	101	480	48.48	74	9.0	"
7	574	115	44	70	100	477	47.70	72	8.8	"
8	577	115	45	69	105	476	49.98	75	9.3	"
9	579	117	46	71	105	476	49.98	74	9.3	"
10	580	119	47	71	109	481	52.43	76	9.7	"
11	579	126	50	74	113	480	54.24	74	10.0	"
12	581	119	47	71	109	490	53.41	77	9.9	"
13	581	120	48	71	109	490	53.41	77	9.9	"
14	594	127	52	75	114	497	56.66	75	10.5	"
15	595	125	52	73	114	503	57.34	77	10.6	"
16	594	129	54	75	112	498	55.78	73	10.3	"
17	583	117	51	64	102	480	48.96	71	9.1	"
18	595	130	52	78	105	495	51.98	67	9.6	"

E

SOLAR CELL ELECTRICAL DATA

CELL DESCRIPTION: HEM Solar Cells (Single Crystal), 2x2 cm, STD Process
SiO AR Coating. Second of Two Sheets

TEST CONDITION: AMO

TEMPERATURE: 25°C Test Block DATE:

NO.	V_{OC} mV	I_{SC} mA	I_{SCB} mA	I_{SCR} mA	I_{Max} mA	V_{Max} mV	P_{Max} mW	CFF %	η %	AREA cm^2
19	598	127	52	75	111	495	54.95	72	10.2	4
20	594	127	51	76	111	490	54.39	72	10.1	"
	CZ control solar cells									
C-1	594	135	53	82	122	500	61.00	76	11.3	4
C-2	593	133	52	81	118	492	58.06	74	10.8	"
C-3	592	133	53	81	120	490	58.80	75	10.9	"
C-4	595	135	54	81	125	500	62.50	78	11.6	"
C-5	592	131	52	79	121	490	59.29	77	11.0	"
*	HEM solar cell Identification.									
	Cell # 1 thru 13 from HEM JPL I.D 1-1214									
	Cell # 14 thru 20 " " " " " 1-1216									

SOLAR CELL ELECTRICAL DATA

CELL DESCRIPTION: HEM Solar Cells (Single Crystal), 2x2 cm, STD Process
SiO AR Coating: Selected Cells For AM1 Measurement.

TEST CONDITION: AM1

TEMPERATURE: 25°C Test Block DATE:

NO.	V_{OC}	I_{SC}	I_{SCB}	I_{SCR}	I_{Max}	V_{Max}	P_{Max}	CFF	n	AREA
	mV	mA	mA	mA	mA	mV	mW	%	%	cm^2
4	575	99			84	476	39.98	70	10.0	4
6	571	98			87	466	40.54	73	10.1	"
11	574	107			96	470	45.12	74	11.3	"
13	575	103			93	470	43.71	74	10.9	"
15	589	108			96	493	47.33	74	11.8	"
17	577	100			86	475	40.85	71	10.2	"
14	541	109			94	486	45.68	71	11.4	"
		6% control Solar cells								
C-1	588	112			104	491	51.06	78	12.8	4
C-2	586	110			100	487	48 70	76	12.2	"